J. Fluid Mech. (1993), *vol.* 247, *pp.* 417–454

Nonlinear effects in the dynamics of shape and volume oscillations for a gas bubble in an external flow

By S. M. YANG,† Z. C. FENG AND L. G. LEAL

Department of Chemical and Nuclear Engineering, University of California – Santa Barbara, Santa Barbara, California, USA

(Received 11 July 1991 and in revised form 1 July 1992)

This paper considers the dynamics of a gas bubble in response to either a pressure pulse or a pressure step at $t = 0$, both in the presence and absence of a mean flow. Our work utilizes small-deformation, domain perturbation analysis carried to second and higher order in the amplitude of deformation, ϵ. In the absence of a mean flow, our analysis of the small deformation problem for an initial *impulsive* perturbation of the bubble volume and shape is closely related to recently published work by Longuet-Higgins on the time-dependent oscillations of an initially deformed bubble in a quiescent fluid. However, in the presence of a mean flow which deforms the bubble, the bubble response to pressure changes is more complex. Specifically, the present analysis identifies a number of different mechanisms for resonant interaction between shape deformation modes and the volume or radial breathing mode of oscillation. This includes not only a fundamental change in the resonant interactions at $O(\epsilon^2)$ – where resonant interaction is also found in the absence of mean flow – but resonant interactions also at the level of $O(\epsilon^{\frac{3}{2}})$ which are not present without the mean flow. On the other hand, the bubble dynamics in response to a *step change* in the pressure distribution in a quiescent fluid exhibits similar resonant interactions at $O(\epsilon^2)$ to those obtained for a pressure pulse in the presence of mean flow because the bubble oscillates around a non-spherical steady-state shape owing to the non-uniform pressure distribution on the bubble surface in both the cases.

1. Introduction

We consider the dynamic response of a bubble to rapid changes in the pressure distribution at the bubble surface, when the bubble is immersed in an inviscid fluid that is either quiescent, or undergoing a steady uniaxial (axisymmetric) straining flow. The deformation of bubbles and drops driven by time-dependent acoustic radiation pressures has been widely studied to investigate such related problems as the fragmentation of oscillating bubbles by instability of the spherical shape, emulsification, and sound propagation in bubbly liquids (cf. Yosioka & Kawasima 1955; Marston & Apfel 1979; Marston 1980; Prosperetti 1984, and others). To describe the bubble oscillations in response to a modulated acoustic pressure on the interface, the disturbance flow field must be determined with the acoustic radiation pressure incorporated into the boundary conditions at the interface. Specifically, we employ the method of domain perturbations to investigate small-amplitude

† Permanent address: Department of Chemical Engineering, Korea Advanced Institute of Science and Technology, Taejon 305-701, Korea.

oscillations of bubble shape and volume, relative to the steady-state configuration in the mean flow. Although the recent development of numerical techniques (e.g. Miksis 1981; Ryskin & Leal 1984; Bach & Hassager 1985; Kang & Leal 1987) has been a very important advance for this type of free-boundary problem, numerical solutions alone are not sufficient because they give only a lumped global picture of the bubble motion. To understand the details of oscillatory motion such as the modal frequencies or the possibility of mode–mode energy transfer mechanisms, we need a complementary analytical study.

Recently, a number of investigators have considered the free oscillations of shape of a compressible gas bubble in a quiescent fluid as a possible source of underwater sound (cf. Plesset & Prosperetti 1977; Hall & Seminara 1980; Prosperetti & Lu 1988; Longuet-Higgins 1989*a–c*, 1990, 1991; Benjamin 1989; Medwin & Beaky 1989; Ffowcs Williams & Guo 1991). Although the quiescent fluid problem is therefore of considerable intrinsic interest, many problems of practical significance involve bubble oscillations with a mean flow at infinity (cf. Subramanyam 1969; Kang & Leal 1988). For example, acoustic noise generation in bubbly liquids almost always involves oscillations of shape or volume with the bubble subjected to some non-trivial mean motion of the suspending fluid.

The interactions between changes of bubble shape, changes of bubble volume, and the mean motion of the surrounding fluid will be shown below to lead to interesting, non-trivial effects. The most closely related existing analysis is due to Longuet-Higgins (1989*a*, 1991) who considered small-amplitude oscillations of an ideal-gas bubble that is initially non-spherical, in a quiescent fluid. In this case, when the frequency of the radial 'breathing' mode of oscillation is twice that of a normal P_n mode of *shape* oscillation (i.e. $\omega_0 = 2\omega_n$), there is a resonant interaction, and the breathing mode gains energy at the expense of the deformation mode, which eventually loses all of its energy to the radial mode. The resulting volume oscillations act as a monopole source of sound.

In the present paper, we consider small amplitude oscillations of shape and volume for an ideal gas bubble that is subjected to an initial pulse or step change in the acoustic radiation pressure at the bubble surface. The inviscid suspending fluid† is assumed either to be initially *quiescent* or to undergo a steady uniaxial flow so that the steady-state bubble shape is non-spherical. We show that there will generally be mode–mode interactions between the radial and shape oscillations, and these interactions can exhibit resonance when the frequency of the radial mode ω_0 is 'matched' with one of the deformation modes. This leads to a slowly varying amplitude envelope for both types of modes and a strong transfer of energy from one type of mode to the other. Similar conclusions were reached by Longuet-Higgins. However, we find that the qualitative details depend critically upon the initial

† In the real, physical system there are a number of mechanisms for energy loss, including viscous dissipation in the liquid, and these will damp both radial and shape oscillations. If the damping occurs on a timescale that is shorter than the slow timescale for modal exchange of energy, no resonant interactions will occur. This fact does not, however, minimize interest in an analytic assessment of the details of modal coupling for the inviscid or non-dissipative limit. A comprehensive study of damping effects requires numerical solution of the full Navier–Stokes problem – the common techniques of simply assigning an *ad hoc* damping term to the modal amplitude equations, or approximating viscous effects as occurring only at the bubble surface, do not seem to be justified (or justifiable) in the present case. It should also be noted that the long timescales characteristic of resonant interactions in the present work are a consequence of the small deformation approximation and will not be relevant to oscillations of finite amplitude. All of these matters are currently being investigated.

conditions – i.e. whether the initial deformed shape occurs owing to a pressure pulse, a pressure step, or is simply imposed (as in Longuet-Higgins' case) in a quiescent fluid. Furthermore, the nature of the interaction and its strength is strongly dependent upon the presence or absence of the ambient extensional flow. In particular, we will show that the flow can interact directly with a deformation mode to enhance the resonant energy transfer from shape to radial oscillation, and, in addition, it produces a self-induced secularity that leads to a modification of the oscillation frequencies.

We begin, in §2, by formulating the governing equations and boundary conditions, and discussing the basic approach to the subsequent analysis. This is followed, in §3, by the steady-state shape for an ideal-gas bubble in an inviscid, axisymmetric extensional flow. In the first part of §4, we analyse the bubble response in a quiescent fluid to an impulse in the pressure at the bubble surface. In the second part of §4, we determine the response in a quiescent fluid to a step change in pressure. Section 5 then examines the bubble response to a pressure impulse when there is a steady mean flow. Our results are summarized in §6.

2. Formulation of the problem

We begin by considering the governing equations and boundary conditions for oscillations of a bubble owing to changes in the pressure distribution at the bubble surface. We assume that the fluid is inviscid with density ρ and that it is undergoing an axisymmetric, uniaxial straining flow far from the bubble.† In the absence of pressure fluctuations or external fluid motion, the pressure is uniform with a magnitude P_0 and the bubble is spherical with an equilibrium radius a. The surface of the bubble is assumed to be clean, mobile and characterized completely by a constant interfacial tension Γ. Finally, we neglect all effects of gravity including the hydrostatic pressure variation in the fluid.

The governing equations appropriate to the problem described above, can be expressed in terms of the velocity potential ϕ and the pressure field P

$$\nabla^2\phi = 0, \tag{2.1}$$

$$\frac{\partial\phi}{\partial t}+\tfrac{1}{2}(\nabla\phi)^2+P = P_0, \tag{2.2}$$

in which the variables are non-dimensional with respect to the characteristic variables: $l_c = a$, $t_c = (a^3\rho/\Gamma)^{\frac{1}{2}}$, $\phi_c = (\Gamma a/\rho)^{\frac{1}{2}}$, and $P_c = \Gamma/a$.

The far-field boundary condition corresponding to the presence of an undisturbed extensional flow with the principal strain rate E can be expressed in terms of the second-order Legendre polynomial $P_2(\eta)$

$$\phi \to \phi^\infty = \tfrac{1}{2}\epsilon^{\frac{1}{3}}r^2P_2(\eta) \quad \text{as } r\to\infty, \tag{2.3}$$

where ϵ is the Weber number, defined as $\epsilon = \rho(Ea)^2a/\Gamma$ and $\eta = \cos\theta$ (see figure 1 for

† Insofar as the analysis in this paper is relevant to understanding the bubble as a source of sound, it should be noted that the assumption of incompressibility is only valid in the vicinity of the bubble. However, as noted by one of the reviewers, and outlined in A. P. Dowing & J. E. Ffowcs Williams (1983), as long as the bubble radius is small compared with the wavelength of sound in the fluid (i.e. the bubble is a 'compact' source), the radiated pressure in the far field is precisely that calculated for an incompressible fluid, but with time being delayed so that t must be replaced by $t-(r-a)/c$.

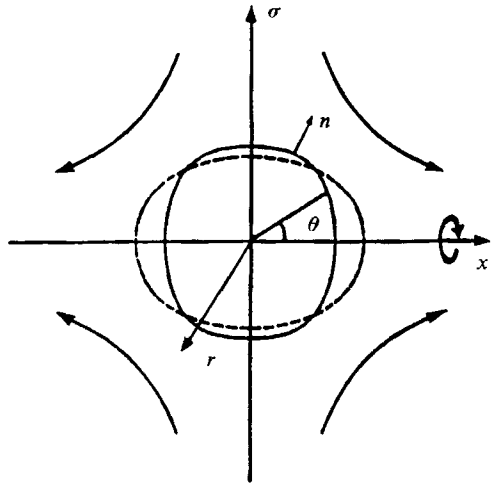

FIGURE 1. An oscillating bubble in a uniaxial straining flow. The x-axis of a cylindrical coordinate system (x, σ, φ) is directed along the axis of symmetry and $|\boldsymbol{x}| = r = (x^2+\sigma^2)^{\frac{1}{2}}$. The strain-rate tensor $\boldsymbol{E}$ has the components $E_{ij} = \frac{1}{2}E(3\delta_{1i}\delta_{1j} - \delta_{ij})$ in the Cartesian coordinate system.

the definition of the coordinate system). The bubble surface is specified in terms of spherical polar coordinates (r, θ, φ), by $S: r - 1 - f(\theta, \varphi, t) = 0$. The kinematic and dynamic boundary conditions *on the bubble surface* thus take the form

$$\frac{\partial S}{\partial t} + \nabla\phi \cdot \nabla S = 0, \tag{2.4}$$

$$\tilde{P} - P_0 - A(\theta, \varphi, t) + \frac{\partial \phi}{\partial t} + \tfrac{1}{2}(\nabla\phi)^2 = \nabla \cdot \boldsymbol{n}, \tag{2.5}$$

where $\tilde{P}$ is the pressure inside the bubble and $\boldsymbol{n}$ is the unit outward normal at the bubble surface. The source of the oscillations in bubble volume and shape is a time- and spatially-dependent pressure at the bubble surface, represented in (2.5) as $A(\theta, \varphi, t)$. This type of surface pressure can be produced experimentally via modulated ultrasonic acoustic wave fields, without producing any net motion of the suspending fluid (cf. Yosioka & Kawasima 1955; Marston 1980).

In addition to the differential equations (2.1) and (2.2) and boundary conditions (2.3)–(2.5), the solution for bubble shape must satisfy an additional constraint on bubble volume, the details of which depend on the properties of the bubble. If we assume that the bubble contains an ideal gas the pressure inside the bubble obeys the perfect gas law

$$\frac{\tilde{P}}{\tilde{P}_0} = \left[\frac{1}{\langle (1+f)^3 \rangle}\right]^{\gamma}, \tag{2.6}$$

in which $\tilde{P}_0$ is the equilibrium pressure for a spherical bubble (i.e. $\tilde{P}_0 - P_0 = 2$ for $f = 0$) and $\langle(\cdot)\rangle$ denotes the spherical surface average of $(\cdot)$. The parameter γ depends on the thermodynamic nature of the bubble oscillation. For an isothermal oscillation γ is unity and for an adiabatic process γ is the ratio of the specific heat capacities ($\gamma = C_p/C_v$; $\gamma = 1.4$ for air). Otherwise γ ranges between these two limiting values.

The problem represented by (2.1)–(2.6) is, of course, both time-dependent and highly nonlinear. One complication is that the boundary conditions (2.4)–(2.5) must

be applied at the bubble surface whose shape is unknown. In the present analysis we utilize the 'domain perturbation' technique for the limit

$$A(\theta, \phi, t) = O(\epsilon) \ll O(1). \tag{2.7}$$

In this technique, we approximate all quantities that are to be evaluated at the surface of the deformed bubble, in terms of equivalent quantities evaluated at the undeformed spherical surface (i.e. $f = 0$) using a Taylor series expansion about $f = 0$, for $\epsilon \ll 1$. Hence, in effect, we replace the original problem, which has boundary conditions at the deformed surface, with an equivalent problem, for $\epsilon \ll 1$, in which modified boundary conditions are applied at the surface of the undeformed (spherical) bubble. As a final simplification, we assume that the applied surface pressure-distribution $A(\theta, \varphi, t)$ is axisymmetric [i.e. $A = A(\theta, t)$] so that the deformed shape of the bubble is also axisymmetric [i.e. $f = f(\theta, t)$].

Based upon the preceding discussion, the kinematic boundary condition (2.4) can be approximated for small ϵ in the form

$$\frac{\partial f}{\partial t} - \frac{\partial \phi}{\partial r} = f\frac{\partial^2 \phi}{\partial r^2} - (1-\eta^2)\left\{\frac{\partial f}{\partial \eta}\frac{\partial \phi}{\partial \eta} + 2f\frac{\partial f}{\partial \eta}\frac{\partial \phi}{\partial \eta} - f\frac{\partial f}{\partial \eta}\frac{\partial^2 \phi}{\partial r\,\partial \eta}\right\} + \tfrac{1}{2}f^2\frac{\partial^3 \phi}{\partial r^3} + O(f^3) \quad \text{at } r = 1. \tag{2.8}$$

Furthermore, the curvature at the bubble surface can be expressed in terms of f as

$$\nabla \cdot \boldsymbol{n} = 2 - 2f + \nabla_s^2 f + 2f^2 + 2f\nabla_s^2 f - 2f^3 - 3f^2\nabla_s^2 f + \left\{\tfrac{3}{2}\nabla_s^2 f + \eta\frac{\partial f}{\partial \eta}\right\}(1-\eta^2)\left(\frac{\partial f}{\partial \eta}\right)^2 + O(f^4), \tag{2.9}$$

where ∇_s^2 denotes the surface Laplacian

$$\nabla_s^2 = \frac{\partial}{\partial \eta}\left\{(1-\eta^2)\frac{\partial}{\partial \eta}\right\}. \tag{2.10}$$

Now, for an ideal-gas bubble, the pressure inside the bubble is determined from the thermodynamic law (2.6). Thus, the dynamic boundary condition (2.5), obtained by using the asymptotic form of (2.6) for $f \ll 1$ and the equilibrium condition ($\tilde{P}_0 - P_0 = 2$), can be expressed in the approximate form

$$\begin{aligned}
&\frac{\partial \phi}{\partial t} + (\nabla_s^2 + 2)f - (\omega_0^2 + 2)\langle f\rangle \\
&= A(\theta, t) - f\frac{\partial^2 \phi}{\partial t\,\partial r} - \tfrac{1}{2}(\nabla\phi)^2 + 2f(f + \nabla_s^2 f) + (\omega_0^2+2)\{\langle f^2\rangle - \tfrac{3}{2}(1+\gamma)\langle f\rangle^2\} \\
&\quad - \tfrac{1}{2}f^2\frac{\partial^3 \phi}{\partial t\,\partial r^2} - f\frac{\partial}{\partial r}(\nabla\phi)\cdot\nabla\phi - f^2(2f + 3\nabla_s^2 f) + (1-\eta^2)\left(\frac{\partial f}{\partial \eta}\right)^2\left\{\tfrac{3}{2}\nabla_s^2 f + \eta\frac{\partial f}{\partial \eta}\right\} \\
&\quad + (\omega_0^2+2)\{\tfrac{1}{3}\langle f^3\rangle - 3(1+\gamma)\langle f\rangle\langle f^2\rangle + \tfrac{3}{2}(\gamma+1)(\gamma+2)\langle f\rangle^3 + O(f^4)\} \quad \text{at } r = 1.
\end{aligned} \tag{2.11}$$

Here ω_0 is the natural frequency of the radial (or so-called 'breathing') mode of oscillation and is defined by

$$\omega_0^2 = 3\gamma\tilde{P}_0 - 2. \tag{2.12}$$

In the present paper, we consider the small deformation limit $\epsilon \ll 1$. In this limit it can be easily seen from (2.2), (2.3), (2.7) and (2.8) that $\phi = O(\epsilon^{\frac{1}{2}})$ and $\partial\phi/\partial t = (\partial\phi/\partial r)_{r=1} = 0$ at $O(\epsilon^{\frac{1}{2}})$. Thus the form of the asymptotic solution that we seek is

$$\phi = \epsilon^{\frac{1}{2}}(\phi_0 + \epsilon^{\frac{1}{2}}\phi_1 + \epsilon\phi_2 + \ldots), \tag{2.13}$$

$$r \equiv 1 + f = 1 + \epsilon f_1 + \epsilon^{\frac{3}{2}} f_2 + \epsilon^2 f_3 + \ldots, \quad \text{at } x \in S. \tag{2.14}$$

We now express the bubble shape function f_j at each order in $\epsilon^{\frac{1}{2}}$ as an infinite series of Legendre polynomials (i.e. surface spherical harmonics in an axisymmetric mode),

$$f_j = \sum_{n=0}^{\infty} a_{j,n}(t) P_n(\eta) \quad (j = 1, 2, \ldots) \tag{2.15}$$

and the velocity potential at each order in $\epsilon^{\frac{1}{2}}$ in terms of solid spherical harmonics (i.e. eigensolutions of the governing equation (2.1)).

$$\phi_j = \begin{cases} \frac{1}{2} r^2 P_2(\eta) + \sum_{n=0}^{\infty} b_{0,n} \dfrac{P_n(\eta)}{r^{n+1}} & (j = 0) \qquad (2.16) \\ \sum_{n=0}^{\infty} b_{j,n}(t) \dfrac{P_n(\eta)}{r^{n+1}} & (j = 1, 2, \ldots). \qquad (2.17) \end{cases}$$

All that remains is to determine the coefficients $a_{j,n}(t)$ and $b_{j,n}(t)$ which satisfy the kinematic and dynamic boundary conditions, (2.8) and (2.11), at the bubble surface.

In the steady-state problem, for a bubble in the flow (2.3) but with $A(\theta, \varphi, t) = 0$, the coefficients $a_{j,n}$ and $b_{j-1,n}$ are constant with $a_{2j,n} = b_{2j-1,n} = 0$ $(j = 1, 2, \ldots)$ (cf. Kang & Leal 1988), and it is straightforward to obtain a solution. We begin with a brief discussion of this steady-state case in the following section.

3. Steady-state solutions

The leading-order approximation to the steady-state problem with $A(\theta, t) = 0$ is the well-known potential flow solution for extensional flow around the undeformed sphere (i.e. $f^{\mathrm{s}} = 0$)

$$\phi_0^{\mathrm{s}} = (\tfrac{1}{2} r^2 + \tfrac{1}{3} r^{-3}) P_2(\eta), \tag{3.1}$$

where the superscript s will be used hereafter to denote the steady-state solution. This solution exactly satisfies the kinematic boundary condition in the form (2.4). However, it cannot satisfy the dynamic boundary condition (2.5) for a spherical bubble; instead, there is a mismatch of $O(\epsilon)$ between the dynamic and capillary pressure distributions at the spherical surface. Thus, the bubble must deform, and we use the domain perturbation technique, summarized by (2.8)–(2.17), to obtain a solution.

To obtain the asymptotic forms of the boundary conditions (2.8) and (2.11) for small $\epsilon \ll 1$, we introduce the expansions (2.13) and (2.14). Then, ϕ_0^{s} given by (3.1) satisfies the leading-order form of the kinematic condition (2.8). The shape correction at $O(\epsilon)$ (i.e. f_1^{s}) is obtained from (3.1) using the leading-order approximation to the dynamic boundary condition (2.11). In particular, if we express f_1^{s} in the form

$$f_1^{\mathrm{s}} = \sum_n a_{1,n}^{\mathrm{s}} P_n(\eta) \tag{3.2}$$

(see 2.15), then it follows from (2.11) that

$$a_{1,0}^{\mathrm{s}} = \begin{cases} \dfrac{5}{12\omega_0^2} & \text{for an ideal-gas bubble,} \\ 0 & \text{for a constant-volume-bubble,} \end{cases}$$

$$a_{1,2}^{\mathrm{s}} = \frac{25}{336}, \quad a_{1,4}^{\mathrm{s}} = -\frac{5}{126}, \quad a_{1,n}^{\mathrm{s}} = 0 \quad (n \neq 0, 2, 4).$$

It may be noted that the volume of an ideal-gas bubble is increased by $O(\omega_0^{-2}\epsilon)$ from the equilibrium value in order to balance the ambient pressure change that is caused by the flow.

The next term in the expansion (2.13) for ϕ^s is $O(\epsilon^{\frac{3}{2}})$, and reflects the change in the flow owing to the change in bubble shape at $O(\epsilon)$. The governing equation for ϕ_2^s comes from the second term in the expansion of the kinematic condition (2.8), with ϕ_0^s and f_1^s given by (3.1) and (3.2). The resulting solution, expressed in the form (2.17), is

$$\phi_2^s = \sum_n b_{2,n}^s \frac{P_n(\eta)}{r^{n+1}}, \tag{3.3}$$

in which

$$b_{2,2}^s = \begin{cases} \dfrac{275}{9072} + \dfrac{25}{36\omega_0^2} & \text{for an ideal-gas bubble,} \\ \dfrac{275}{9072} & \text{for a constant-volume bubble,} \end{cases}$$

$$b_{2,4}^s = \frac{325}{5544}, \quad b_{2,6}^s = -\frac{125}{4158}, \quad b_{2,n}^s = 0 \quad (n \neq 2,4,6).$$

Following the preceding analysis, the second correction at $O(\epsilon^2)$ to the bubble shape is then obtained from (2.11). For an ideal-gas bubble, the result can be expressed in the form

$$f_3^s = \sum_n a_{3,n}^s P_n(\eta) \tag{3.4}$$

in which

$$a_{3,0}^s = -\frac{25}{144}\left\{\frac{67}{9072} - \frac{11}{63\omega_0^2} - \frac{3\gamma+5}{2\omega_0^4} - \frac{3\gamma-1}{\omega_0^6}\right\},$$

$$a_{3,2}^s = \frac{125}{1008}\left\{\frac{20011}{99792} + \frac{1}{\omega_0^2}\right\}, \quad a_{3,4}^s = -\frac{25}{378}\left\{\frac{469163}{6342336} + \frac{1}{\omega_0^2}\right\},$$

$$a_{3,6}^s = -\frac{199075}{39517632}, \quad a_{3,8}^s = \frac{2725}{1459458}, \quad a_{3,n}^s = 0 \quad (n \neq 0,2,4,6,8).$$

For a constant-volume bubble, the corresponding coefficients $a_{3,n}^s$ $(n = 0,2,4,6,8)$ can be obtained by taking the limit $\omega_0^2 \to \infty$ in the above solution. Higher-order approximations for ϕ^s and f^s could be obtained by a straightforward continuation of the same procedure. However, the solution obtained above is sufficient for present purposes.

If we summarize our results, we have shown that the shape function up to $O(\epsilon^2)$ is given in the form

$$r = 1 + \epsilon \sum_n a_{1,n}^s P_n(\eta) + \epsilon^2 \sum_n a_{3,n}^s P_n(\eta) + O(\epsilon^3). \tag{3.5}$$

For the limiting case of a constant-volume bubble (i.e. $\omega_0^2 \to \infty$), this solution is exactly the same as obtained by Miksis (1981) and Kang & Leal (1988). As noted in those earlier papers, the bubble shape is not ellipsoidal at the leading order of approximation, but exhibits a maximum radius at $\theta = \frac{1}{6}\pi$ which clearly indicates a barrel-like shape. It can be seen from the present analysis that this rather surprising feature is independent of the compressibility of the bubble.

The solution (3.5) also suggests the presence of a limit point at a critical Weber number $\epsilon = \epsilon_c$ for existence of steady solutions on the branch that includes the

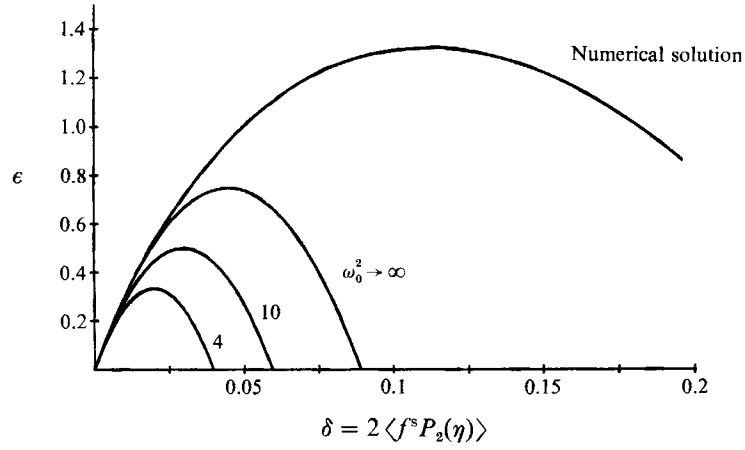

FIGURE 2. Perturbation solutions for steady-state shape as a function of the magnitude of the P_2 mode of deformation δ. Also shown is the numerical solution of Miksis (1981) and Ryskin & Leal (1984) for $\omega_0^2 \to \infty$.

spherical shape in the absence of a flow. Indeed, following Kang & Leal (1988), an estimate of the critical Weber number can be obtained by transforming the ϵ-perturbation into a P_2-perturbation in which the small parameter is the magnitude of the $P_2(\eta)$ mode of deformation,

$$\delta = 2\langle f^s P_2(\eta)\rangle, \tag{3.6}$$

instead of ϵ. In this way, the limit point which appears as a singular point on the stable solution branch at a critical Weber number ϵ_c is transformed to a regular point, and we can determine the Weber number ϵ as a function of δ for both the unstable and stable parts of the solution curve. The result up to $O(\delta^2)$ can be expressed in the form

$$\epsilon = c_1\delta + c_2\delta^2 + O(\delta^3), \tag{3.7}$$

in which

$$c_1 = \frac{5}{2a^s_{1,2}}, \quad c_2 = -\frac{25a^s_{3,2}}{4(a^s_{1,2})^3}.$$

The critical Weber number, which occurs when $\partial\epsilon/\partial\delta = 0$, can thus be estimated as

$$\epsilon_c = \frac{a^s_{1,2}}{4a^s_{3,2}} \quad \text{at} \quad \delta_c = \frac{(a^s_{1,2})^2}{5a^s_{3,2}}. \tag{3.8}$$

The critical value for a constant-volume bubble (i.e. $\omega_0^2 \to \infty$) is 0.7480 which is identical to the result obtained by Kang & Leal (1988). As noted in the earlier paper, this estimate of the critical Weber number at which the stability of the solution branch is exchanged is substantially below the value 1.38 obtained numerically for an incompressible bubble by Miksis (1981) and Ryskin & Leal (1984).

In figure 2, the Weber number ϵ is plotted as a function of δ from equation (3.7) for three values of $\omega_0^2 = 4$, 10 and ∞. Also included for comparison is the numerical result of Miksis (1981) and Ryskin & Leal (1984) for a constant-volume bubble (i.e. $\omega_0^2 \to \infty$). Although the critical Weber number predicted by the P_2-perturbation solution is considerably below the value obtained numerically, we can see that the general features of the solution are more or less the same. It can be easily seen from figure 2 that the maximum value of the Weber number for the existence of a stable steady-state solution is monotonically increased as ω_0 increases. (The critical value

for $\omega_0^2 = 4$ is $\epsilon_c = 0.3329$, and the value for $\omega_0^2 = 10$ is $\epsilon_c = 0.4991$.) Thus, the gas bubble becomes less stable as the compressibility increases owing to the increased bubble volume that is required to balance the ambient pressure change indueed by the external mean flow.

4. Small-amplitude oscillation of an ideal-gas bubble in a quiescent fluid

In this and the following section we consider the oscillations of volume and shape that occur for an initially spherical, equilibrium bubble in response to an asymptotically small, but abrupt change in the ambient pressure distribution at the bubble surface.

Longuet-Higgins (1991) considered the related problem in which an ideal-gas bubble exhibits a spontaneous shape oscillation, beginning at $t = 0$ with the fluid at rest, and an initial *perturbation in shape* at $O(\epsilon)$. The corresponding initial conditions expressed in terms of the coefficients $a_{j,n}(t)$ of the shape function (2.15) are

$$\left.\begin{aligned} a_{1,0}(0) = 0, \quad a_{1,n}(0) = 1, \quad \frac{\partial a_{1,0}(0)}{\partial t} = \frac{\partial a_{1,n}(0)}{\partial t} = 0, \\ a_{2,0}(0) = -\frac{1}{2n+1}, \quad a_{2,n}(0) = 0, \quad \frac{\partial a_{2,0}(0)}{\partial t} = \frac{\partial a_{2,n}(0)}{\partial t} = 0. \end{aligned}\right\} \tag{4.1}$$

Longuet-Higgins (1991) found, in this case, that when the radial breathing mode has twice the frequency of a normal mode of shape deformation (i.e. $\omega_0 = 2\omega_n$), there is a resonant interaction at $O(\epsilon^2)$ and the breathing mode gains energy at the expense of the shape deformation mode. In fact, in the case considered by Longuet-Higgins, the shape deformation eventually loses all of its energy to the radial mode of oscillation.

However, we shall see from the calculations below that the details of mode–mode interactions can be quite different when the initial deformation process occurs as a consequence of an abrupt change in the 'radiation' pressure at the bubble surface rather than passively, as in the Longuet-Higgins analysis. In this section we consider small-amplitude oscillations of an ideal-gas bubble in response to both an impulsive change and a step change in this pressure.

4.1. *Impulsive response in a quiescent fluid*

Let us begin by considering the bubble response in a *quiescent* fluid to an *impulse* in the pressure at the bubble surface. For this case, the function $A(\theta, t)$ can be expressed in terms of the Legendre polynomials $P_n(\eta)$ for an axisymmetric mode:

$$A(\theta, t) = \epsilon \sum_n A_n \delta(t) P_n(\eta), \tag{4.2}$$

where ϵA_n is the impulse magnitude of the $P_n(\eta)$ mode and $\delta(t)$ is the Dirac-delta function. To begin with, it is obvious, in the absence of an external mean flow (i.e. $\phi_0 = 0$ in the solution (2.13)), that $f_{2j} = \phi_{2j} = 0$ $(j = 1, 2, 3, \ldots)$ in the expansions (2.13) and (2.14) and $a_{2j,n}(t) = b_{2j,n}(t) = 0$ $(j = 1, 2, \ldots)$ in the normal forms of (2.15)–(2.17). The equation of motion and boundary conditions for the linear approximation at $O(\epsilon)$ admit solutions in the form of normal modes

$$a_{1,n}(t) = -\frac{(n+1)A_n}{\omega_n} \sin \omega_n t, \tag{4.3}$$

$$\phi_{1,n}(t, r, \eta) = A_n \frac{1}{r^{n+1}} P_n(\eta) \cos \omega_n t, \tag{4.4}$$

for $n = 0, 1, 2, \ldots$. Here, $\omega_0 (n = 0)$ is defined in (2.12) for the radial mode of oscillation and ω_n is defined as

$$\omega_n^2 = (n-1)(n+1)(n+2) \tag{4.5}$$

for a deformation mode. Thus, the problem can be viewed as an initial-value problem with

$$a_{j,n}(0) = 0, \quad \frac{\partial}{\partial t} a_{1,n}(0) = -(n+1) A_n, \quad \frac{\partial}{\partial t} a_{j+1,n}(0) = 0 \quad (j = 1, 2, \ldots) \tag{4.6}$$

in a time-independent ambient pressure field (cf. (4.1) for the Longuet-Higgins (1991) problem).

Consider now the second approximation which occurs at $O(\epsilon^2)$ in the quiescent fluid. [In the presence of the linear extensional flow, the second approximation will be shown later to occur at $O(\epsilon^{\frac{3}{2}})$.] On substituting $a_{1,n}$ (i.e. f_1) and $\phi_{1,n}$ into the kinematic and dynamic boundary conditions (2.8) and (2.11), we have

$$\frac{\partial^2 a_{3,0}}{\partial t^2} + \omega_0^2 a_{3,0} = -\frac{A_0^2}{4\omega_0^2}\{3(\gamma+2)\omega_0^2 + 2(3\gamma-1)\}\cos 2\omega_0 t + \frac{A_0^2}{4\omega_0^2}\{3\gamma\omega_0^2 + 2(3\gamma-1)\}$$
$$- \frac{(n+1)^2 A_n^2}{4\omega_n^2(2n+1)}\left\{\frac{4n+9}{n+1}\omega_n^2 - 2\omega_0^2\right\}\cos 2\omega_n t - \frac{(n+1)^2 A_n^2}{4\omega_n^2(2n+1)}\left\{\frac{3\omega_n^2}{n+1} - 2\omega_0^2\right\}, \tag{4.7}$$

$$b_{3,0}(t) = 2a_{1,0} b_{1,0} + \frac{2(n+1)}{2n+1} a_{1,n} b_{1,n} - \frac{\partial a_{3,0}}{\partial t} \tag{4.8}$$

for the amplitude of the radial mode of oscillation. A similar expression can also be obtained in a straightforward way for the amplitude of any of the deformation modes. It can be seen from (4.7) that when $\omega_0 = 2\omega_n$ there are secular terms on the right-hand side, which indicate a resonant interaction between the radial mode and the $P_n(\eta)$-mode of deformation. Since we expect bounded solutions for the various shape modes (recall that the pressure change is small, of $O(\epsilon)$), it is evident that the form of the solution (4.3) is overly simplified. In particular, to avoid the secularity at $O(\epsilon^2)$ when $\omega_0 = 2\omega_n$ we must employ a two-timing expansion in which the amplitude and phase of the $O(\epsilon)$ modes are assumed to exhibit a slow variation, superposed on the rapid oscillations described by (4.3) and (4.4).

Before considering the details of the resonant case, however, let us first consider the solutions of (4.7) and (4.8) for the non-resonant case ($\omega_0 \neq 2\omega_n$). In this case, solutions for $a_{3,0}$ and $b_{3,0}$ can be easily determined which satisfy the initial condition (4.6). The known solutions for $a_{j,0}, b_{j,0}$ $(j = 1, 3)$ can then be used to evaluate the corresponding pressure disturbance at large distances r using

$$P^\infty = -\epsilon\left[\frac{\partial \phi_1}{\partial t} + \epsilon\left\{\frac{\partial \phi_3}{\partial t} + \tfrac{1}{2}(\nabla\phi_1)^2\right\}\right] + O(\epsilon^3). \tag{4.9}$$

In particular, as $r \to \infty$, we find

$$P^\infty \sim -\left(\epsilon\frac{\partial b_{1,0}}{\partial t} + \epsilon^2\frac{\partial b_{3,0}}{\partial t}\right)\frac{1}{r},$$

or

$$rP^\infty = \epsilon A_0 \omega_0 \sin\omega_0 t + \epsilon^2\left[\frac{A_0^2}{2\omega_0^2}\{(2\gamma+1)\omega_0^2 + \tfrac{4}{3}(3\gamma-1)\}\cos\omega_0 t\right.$$
$$+ \frac{(n+1)A_n^2}{4(2n+1)}\left\{3 + \frac{(4n-1)\omega_0^2}{\omega_0^2 - 4\omega_n^2}\right\}\cos\omega_0 t - \frac{A_0^2}{\omega_0^2}\{\gamma\omega_0^2 + (2\gamma - \tfrac{2}{3})\}\cos 2\omega_0 t$$
$$\left. - \frac{(n+1)(4n-1)\omega_n^2 A_n^2}{(2n+1)(\omega_0^2 - 4\omega_n^2)}\cos 2\omega_n t\right] \quad \text{as } r \to \infty. \tag{4.10}$$

It can be seen that the distortion mode at $O(\epsilon)$, without the radial mode of oscillation at $O(\epsilon)$ (i.e. with $A_0 = 0$) only emits a monopole-like contribution at $O(\epsilon^2)$. This contribution is due to the change in bubble volume.

Two important conclusions can be drawn from the solution (4.10) when $A_0 = 0$ (i.e. the ambient pressure impulse has no radially symmetric component). First, the induced monopole pressure disturbance in this case has two oscillatory components; one with the frequency of the zero-order breathing mode and the other with a frequency double that of the linear mode of deformation ω_n. Both of these terms have an amplitude proportional to the square of the intensity of the pressure impulse, A_n^2. Secondly, if we examine the order of magnitude of these terms, we see that the amplitude can be surprisingly large, especially as $\omega_0 \to 2\omega_n$. As shown previously in the closely related problem analysed by Longuet-Higgins, the mode–mode interactions in this limit become resonant, and we must employ a two-timing procedure to obtain a valid (bounded) solution.

Let us then turn to the special case $\omega_0 = 2\omega_n$ in which the radial and P_n deformation modes are in exact resonance. As we have already noted, secular terms appear in the governing equations at $O(\epsilon^2)$, so that the solution at $O(\epsilon)$ for this case must be expressed in the form of normal modes with a slowly varying amplitude,

$$a_{1,n}(t,\tau) = \tfrac{1}{2}\{\alpha_{1,n}(\tau)\exp(\mathrm{i}\omega_n t)\} + \text{c.c.}, \tag{4.11}$$

$$b_{1,n}(t,\tau) = -\frac{\mathrm{i}\omega_n}{2(n+1)}\alpha_{1,n}(\tau)\exp(\mathrm{i}\omega_n t) + \text{c.c.}, \tag{4.12}$$

with

$$\alpha_{1,n}(0) = \frac{A_n(n+1)\,\mathrm{i}}{\omega_n}. \tag{4.13}$$

(In (4.11) and (4.12) c.c. signifies the complex conjugate.) The slowly varying complex functions $\alpha_{1,n}(\tau)$ are determined from the condition that no secular terms appear in (4.7) and (4.8). After some manipulation, the conditions for the absence of secular behaviour can be shown to take the form

$$\frac{\mathrm{d}\alpha_{1,0}}{\mathrm{d}\tau} = \mathrm{i}H_5\,\alpha_{1,n}^2, \tag{4.14}$$

$$\frac{\mathrm{d}\alpha_{1,n}}{\mathrm{d}\tau} = \mathrm{i}H_6\,\alpha_{1,0}\,\alpha_{1,n}^*, \tag{4.15}$$

where

$$H_5 = \frac{(4n-1)\,\omega_n}{16(n+1)(2n+1)}, \quad H_6 = \frac{(4n-1)}{4}\omega_n,$$

and the superscript * denotes the complex conjugate. The initial conditions are given in (4.13).

To solve (4.14) and (4.15), we can use a polar decomposition of the form

$$\alpha_{1,0} = M_0(\tau)\exp(\mathrm{i}\Theta_0\tau), \quad \alpha_{1,n} = M_n(\tau)\exp(\mathrm{i}\Theta_n\tau). \tag{4.16}$$

Here, M_0 and M_n are the amplitude functions, while $\Theta_0(\tau)$ and $\Theta_n(\tau)$ represent the phase shift. Note that if Θ_0 and Θ_n depend linearly on τ, the phase shift corresponds to a simple change in the oscillation frequency. Upon substituting (4.16) into (4.14) and (4.15), we obtain

$$\frac{\mathrm{d}M_0}{\mathrm{d}\tau} = -H_5 M_n^2 \sin(2\Theta_n - \Theta_0), \tag{4.17a}$$

$$M_0 \frac{d\Theta_0}{d\tau} = H_5 M_n^2 \cos(2\Theta_n - \Theta_0), \tag{4.17b}$$

$$\frac{dM_n}{d\tau} = H_6 M_0 M_n \sin(2\Theta_n - \Theta_0), \tag{4.17c}$$

$$\frac{d\Theta_n}{d\tau} = H_6 M_0 \cos(2\Theta_n - \Theta_0). \tag{4.17d}$$

The initial conditions corresponding to (4.13) are

$$\Theta_0 = \Theta_n = \tfrac{1}{2}\pi, \quad M_0 = \frac{A_0}{\omega_0}, \quad M_n = \frac{(n+1)A_n}{\omega_n}. \tag{4.18}$$

With these initial conditions,

$$\frac{d\Theta_0}{d\tau} = \frac{d\Theta_n}{d\tau} = 0 \quad \text{at } \tau = 0$$

and thus $\Theta_0 = \Theta_n = \frac{1}{2}\pi$ for all τ. In this case,

$$\frac{dM_0}{d\tau} = -H_5 M_n, \quad \frac{dM_n}{d\tau} = H_6 M_0 M_n. \tag{4.19}$$

The energy equation for the oscillation described by (4.19) can easily be shown to satisfy

$$H_6 M_0^2(\tau) + H_5 M_n^2(\tau) = \text{const.} \tag{4.20}$$

Any solution of (4.19) must satisfy this constraint. (Note that if $A_n = 0, A_0 \neq 0$, then $dM_0/d\tau$ and $dM_n/d\tau$ are both zero at $\tau = 0$. In this case, there is no coupling between modes, and the bubble simply undergoes volume oscillations of constant amplitude A_0/ω_0 with frequency ω_0.)

With the equations in the form (4.19), an analytic solution is easily obtained. This solution, expressed in terms of $\alpha_{1,0}$ and $\alpha_{1,n}$, takes the form

$$\alpha_{1,0}(\tau) = i\beta_{1,0}(\tau) = -R_n \, i \tanh(U_n \tau + V_n), \tag{4.21}$$

$$\alpha_{1,n}(\tau) = i\beta_{1,n}(\tau) = T_n \, i \operatorname{sech}(U_n \tau + V_n) \quad (n \geqslant 2). \tag{4.22}$$

The coefficients R_n, T_n, U_n and V_n are

$$R_n = \text{Sign}\{A_0\}\left(\frac{(n+1)A_n^2 + (2n+1)A_0^2}{\omega_0^2(2n+1)}\right)^{\frac{1}{2}}$$

$$T_n = \text{Sign}\{A_n\}\left(\frac{(n+1)A_n^2 + (2n+1)A_0^2}{(n-1)(n+2)}\right)^{\frac{1}{2}}$$

$$U_n = \text{Sign}\{A_0\}\tfrac{1}{8}(4n-1)\left(\frac{(n+1)A_n^2 + (2n+1)A_0^2}{2n+1}\right)^{\frac{1}{2}}$$

and

$$V_n = -\sinh^{-1}\left(\left(\frac{A_0^2(2n+1)}{A_n^2(n+1)}\right)^{\frac{1}{2}}\right),$$

in which $\text{Sign}\{x\} = x/|x|$.

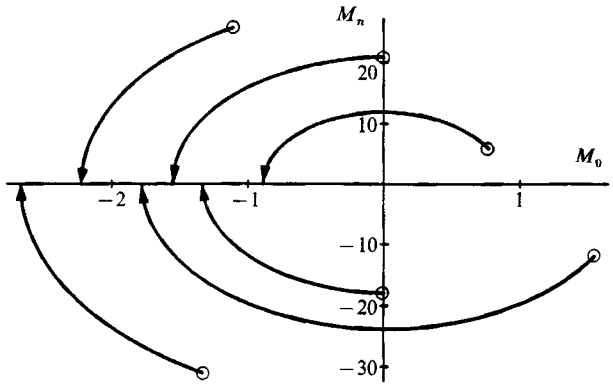

FIGURE 3. Phase diagram, M_n *vs.* M_0, for the resonant case $\omega_0 = 2\omega_4$ for various sets of initial conditions $\{M_0(0), M_4(0)\}$: ○, initial points in the phase portrait.

By applying the initial conditions (4.1), instead of (4.6) for the present case, the solution for Longuet-Higgins' (1991) problem can be readily reproduced in the same form as (4.21) and (4.22):

$$\alpha_{1,0}(\tau) = \mathrm{i}\frac{4n-1}{16((2n+1)(n+1))^{\frac{1}{2}}}\tanh\left[\tfrac{1}{8}(4n+1)\left(\frac{(n-1)(n+2)}{(2n+1)}\right)^{\frac{1}{2}}\tau\right], \tag{4.23}$$

$$\alpha_{1,n}(\tau) = \operatorname{sech}\left[\tfrac{1}{8}(4n-1)\left(\frac{(n-1)(n+2)}{(2n+1)}\right)^{\frac{1}{2}}\tau\right]. \tag{4.24}$$

Since Θ_0 and Θ_n are independent of time, τ, it can be seen from (4.11)–(4.13), in conjunction with (4.16), that the mode–mode resonance at $O(\epsilon^2)$ generates a slowly varying amplitude envelope for the shape and volume modes of oscillation at $O(\epsilon)$. The phase-plane portrait of this oscillatory behaviour is shown in figure 3. As indicated by (4.20), the trajectories of M_0 versus M_n are closed ellipses corresponding to different constants on the right-hand side of (4.20).

It will be noted from (4.19) that both $\mathrm{d}M_0/\mathrm{d}\tau$ and $\mathrm{d}M_n/\mathrm{d}\tau = 0$ when $M_n = 0$. Thus, for any given pair of initial values for M_0 and M_n, the solution will follow one of the solution trajectories of figure 3, but in every case, this leads asymptotically to a final state in which $M_n = 0$ and $M_0 \neq 0$. In other words, the resonant interactions at $O(\epsilon^2)$ produce an exchange of energy between the shape and radial modes at $O(\epsilon)$, which occurs on a timescale ϵt, and leads finally to a one-way transfer of all of the initial deformation energy to the radial mode. This qualitative feature of the energy transfer between modes is identical to Longuet-Higgins (1991) solution, (4.23) and (4.24), for bubble oscillation from an initially distorted shape with equilibrium volume.

It can be seen from figure 3, that the details of the energy transfer process depend on the magnitude and signs of M_0 and M_n at $t = 0$, as given by (4.18). In particular, if we start with an initial state in the upper right or lower right quadrants of figure 3, the magnitude of the radial mode will first decrease as energy is transferred to the deformation mode, until eventually the radial mode vanishes altogether, and the magnitude of the deformation mode is at a peak. Beyond this point in time, however, the energy transfer goes back in the opposite direction, with the radial mode growing and the deformation mode decaying until eventually all of the energy resides permanently in the radial mode. If the initial state is in the upper-left or lower-left

quadrant, on the other hand, the energy transfer will be from the deformation mode to the radial mode at all times, exactly following the second part of the dynamics described above. Thus, it can be seen from the definitions of R_n and T_n (following (4.21) and (4.22)), that the energy transfer direction is initially sensitive to the signs of A_0 and A_n, but eventually all of the energy resides in the radial mode.

At the resonant state, the monopole pressure distribution can be determined by utilizing the equation of motion, correct to $O(\epsilon^2)$. The calculated disturbance pressure at large distances from the bubble is given by

$$P^{\infty} = \epsilon\{4\omega_n^2 \beta_{1,0}(\tau)\sin 2\omega_n t\}\frac{1}{r} + \epsilon^2\omega_n^2\left[\left\{\frac{(12n+9)}{4(2n+1)(n+1)}\beta_{1,n}^2 - \frac{(8n+5)(n+1)}{4(2n+1)\omega_n^2}A_n^2 + \frac{(2\gamma+1)\omega_n^2+(\gamma-\frac{1}{3})}{2\omega_n^4}A_0^2\right\}\cos 2\omega_n t - \beta_{1,0}^2\left\{4\gamma+(2\gamma-\tfrac{2}{3})\frac{1}{\omega_n^2}\right\}\cos 4\omega_n t\right]\frac{1}{r}. \quad (4.25)$$

Comparing (4.25) with the form of the amplitude function $a_{1,0} = -\beta_{1,0}(\tau)\sin\omega_0 t$, it can be seen that the leading-order contribution to the monopole-like pressure oscillation is in anti-phase with the breathing mode oscillation, and the intensity of the monopole radiation is initially increased or decreased depending on the sign of A_0. (If $A_0 > 0$ it decreases, and vice versa.) However, again as $t \to \infty$, the amplitude of the monopole-like contribution is increased at the expense of the exponentially decaying deformation mode (see figure 3).

4.2. *Step response in a quiescent fluid*

We have seen in the preceding section that the bubble response to an impulse in pressure in the absence of an external flow involves a resonant interaction between the radial breathing mode and the P_n-mode of deformation when $\omega_0 = 2\omega_n$, which leads eventually to the one-way transfer of energy at $O(\epsilon)$, from the deformation mode to the radial mode of oscillation. The same one-way transfer is also found in the related problem of Longuet-Higgins. An obvious question is whether resonant mode–mode interactions always transfer energy to the radial mode at long times.

In order to investigate the factors which govern the direction of energy transfer, it is advantageous to consider a second problem of a bubble in a quiescent fluid, but with the pressure at the bubble surface undergoing a step change at $t = 0$ instead of an impulse, i.e.

$$A(\theta, t) = \sum_n \epsilon A_n H(t) P_n(\eta). \quad (4.26)$$

Here, $H(t)$ is the Heaviside step function. The reason for our interest in this problem will become evident after we have completed the analysis. Anticipating the appearance of secular terms at $O(\epsilon^2)$, we begin by writing the $O(\epsilon)$ solutions as

$$a_{1,0}(t,\tau) = \frac{1}{2}\left[\alpha_{1,0}(\tau)\exp(\mathrm{i}\omega_0 t) - \frac{A_0}{\omega_0^2}\right] + \text{c.c.}, \quad (4.27)$$

$$a_{1,n}(t,\tau) = \frac{1}{2}\left[\alpha_{1,n}(\tau)\exp(\mathrm{i}\omega_n t) - \frac{(n+1)A_n}{\omega_n^2}\right] + \text{c.c.}, \quad (4.28)$$

$$\phi_{1,n}(t,\tau,r,\eta) = -\frac{\mathrm{i}\omega_n}{2(n+1)}\alpha_{1,n}(\tau)\exp(\mathrm{i}\omega_n t)\frac{P_n(\eta)}{r^{n+1}} + \text{c.c.}, \quad (4.29)$$

$$\alpha_{1,n}(0) = \frac{(n+1)A_n}{\omega_n^2}. \quad (4.30)$$

These expressions clearly satisfy the initial condition ($a_{j,n} = 0$ and $\partial a_{j,n}/\partial t = 0$ at $t = 0$) and the condition for imposition of a step change in the ambient pressure. It can be noted from (4.27)–(4.30) that an ideal-gas bubble will execute both radial and shape oscillations around a 'new' steady-state radius and shape,

$$r = 1 - \epsilon\left[\frac{A_0}{\omega_0^2} + \sum_{n=2} (n+1)\frac{A_n}{\omega_n^2} P_n\right],$$

in response to the step change in the pressure distribution on the bubble surface. This transition of the base-state from the initial equilibrium shape and volume leads to major changes in the bubble dynamics as we shall see shortly. To obtain governing equations for the slowly varying coefficients $\alpha_{1,n}(\tau)$, we require the governing equations for the $O(\epsilon^2)$ terms in the expansions (2.13) and (2.14).

By substituting the general solution forms (4.27)–(4.30) into the kinematic and dynamic boundary conditions, (2.8) and (2.11), we find

$$\begin{aligned}\frac{\partial^2}{\partial t^2} a_{3,0} + \omega_0^2 \alpha_{3,0} = &-\mathrm{i}\omega_0 \frac{\mathrm{d}\alpha_{1,0}}{\mathrm{d}\tau} \exp(\mathrm{i}\omega_0 t) + \frac{A_n \alpha_{1,n}}{2(2n+1)\omega_n^2}\{2\omega_0^2(n+1) - \omega_n^2(n+5)\}\exp(\mathrm{i}\omega_n t) \\ &+ \frac{\alpha_{1,n}^2}{8(2n+1)}\left\{\frac{4n+9}{n+1}\omega_n^2 - 2\omega_0^2\right\}\exp(2\mathrm{i}\omega_n t) \\ &+ \left\{\frac{1-3\gamma}{\omega_0^2} - \frac{2+3\gamma}{2}\right\} A_0 \alpha_{1,0} \exp(\mathrm{i}\omega_0 t) \\ &+ \text{c.c.} + \text{non-secular terms}, \end{aligned} \tag{4.31}$$

$$\begin{aligned}\frac{\partial^2}{\partial t^2} a_{3,n} + \omega_n^2 a_{3,n} = &-\mathrm{i}\omega_n \frac{\mathrm{d}\alpha_{1,n}}{\mathrm{d}\tau} \exp(\mathrm{i}\omega_n t) + \frac{A_n(n+1)\alpha_{1,0}}{2\omega_n^2}\{\omega_0^2(n-1) - 2\omega_n^2\}\exp(\mathrm{i}\omega_0 t) \\ &+ \tfrac{1}{4}(\alpha_{1,0}\alpha_{1,n}^*)\{3\omega_n^2 - 3\omega_n\omega_0 - (n-1)\omega_0^2\}\exp(\mathrm{i}(\omega_0 - \omega_n)t) \\ &- \left[\frac{3}{2}\frac{\omega_n^2}{\omega_0^2} A_0 + \frac{(2n+1)(n+1)K_n}{3n+1}\left[\frac{2(n+1)}{\omega_n^2} + \frac{10-n}{4}\right] A_n\right]\alpha_{1,n}\exp(\mathrm{i}\omega_n t) \\ &+ \text{c.c.} + \text{non-secular terms}, \end{aligned} \tag{4.32}$$

with $$K_n \equiv \left[\frac{(n-1)!!}{(n/2)!}\right]^3 \frac{(\frac{3}{2}n)!}{(3n-1)!!}, \; n \text{ even}; \quad K_n \equiv 0, \; n \text{ odd}.$$

Upon examination, it can easily be seen that secular terms exist in (4.31) and (4.32), both for $\omega_0 = 2\omega_n$ and $\omega_0 = \omega_n$. Hence, in this case, the radial mode can be in resonance with the P_n mode of deformation ($n \neq 0$) for either $\omega_0 = \omega_n$ or $\omega_0 = 2\omega_n$. Furthermore, both (4.31) and (4.32) contain additional secular terms of the self-induced type, which are present for all values of ω_0 and ω_n. As is well known, such terms do not result from mode–mode interactions, but rather represent a shift in the frequency of oscillation. In the present case, there are self-induced terms proportional to A_0 in both (4.31) and (4.32), and these correspond to a frequency shift due to the change in bubble volume caused by the step increase or decrease in the spherically symmetric pressure contribution at the bubble surface. In addition, for n even, there is also a frequency shift in the shape deformation modes due to the change in mean bubble shape for $A_n \neq 0$.

Thus, prior to discussing the two cases of resonance between the radial and shape deformation modes, we briefly consider the frequency shift for non-resonant values

of ω_0 and ω_n. This can be derived easily from (4.31) and (4.32). In particular, the conditions to eliminate the self-induced secularity can be seen to be

$$\frac{\mathrm{d}\alpha_{1,0}}{\mathrm{d}\tau} = \mathrm{i}H_2\alpha_{1,0}, \tag{4.33}$$

$$\frac{\mathrm{d}\alpha_{1,n}}{\mathrm{d}\tau} = iH_4\alpha_{1,n}, \tag{4.34}$$

where

$$H_2 \equiv \left(\frac{2+3\gamma}{2\omega_0}+\frac{3\gamma-1}{\omega_0^3}\right)A_0, \quad H_4 = \frac{3\omega_n}{2\omega_0^2}A_0+\frac{(2n+1)(n+1)K_n}{(3n+1)\omega_n}\left[\frac{2(n+1)}{\omega_n^2}+\frac{10-n}{4}\right]A_n. \tag{4.35}$$

Thus

$$\alpha_{1,0} = \frac{A_0}{\omega_0^2}\exp(\mathrm{i}H_2\tau), \quad \alpha_{1,n} = \frac{(n+1)A_n}{\omega_n^2}\exp(\mathrm{i}H_4\tau), \tag{4.36}$$

and it follows that

$$\left.\begin{aligned} a_{1,0}(t) &= \frac{A_0}{\omega_0^2}\left[\cos\left\{\omega_0\left(1+\frac{\epsilon A_0}{\omega_0^2}\left(\frac{2+3\gamma}{2}+\frac{3\gamma-1}{\omega_0^2}\right)\right)t\right\}-1\right], \\ a_{1,n}(t) &= \frac{n+1}{\omega_n^2}A_n\left[\cos\left\{\omega_n\left(1+\epsilon\frac{H_4}{\omega_n}\right)t\right\}-1\right]. \end{aligned}\right\} \tag{4.37}$$

Hence, the frequency of both volume and shape oscillations is modified by the change in mean volume induced by a step change in the isotropic pressure. Furthermore, the frequency of shape oscillations is additionally modified by the change in mean shape that accompanies a step change in the non-isotropic surface pressure.

The frequency change for volume oscillations is either positive or negative depending on the sign of A_0. When $A_0 < 0$, the bubble volume increases from the equilibrium value, which results in a decrease in oscillation frequency. This decrease in frequency has an important significance, because at a critical magnitude of the step change in pressure at the bubble surface, $-(\epsilon A_0)_c$, the square of the true frequency of oscillation becomes zero and eigenvalues for the coefficient function $a_{1,0}$ change from pure imaginary to real. The critical intensity, $-(\epsilon A_0)_c$, where this occurs will thus correspond exactly to a limit point for existence of a steady-state value for the bubble radius in the reduced surface pressure field, i.e. $r = 1-\epsilon A_0/\omega_0^2$. An estimate of the critical intensity can be obtained from the present asymptotic solution (4.37):

$$(-\epsilon A_0)_c = \frac{\omega_0^4}{(2+3\gamma)\omega_0^2+2(3\gamma-1)}. \tag{4.38}$$

Thus, as the compressibility of the bubble increases (i.e. ω_0^2 decreases), the gas bubble becomes less stable to a step change in the pressure at its surface. It can be seen from (4.37) that when $A_0 > 0$, the bubble volume decreases and the bubble oscillates with increased frequency around the 'new' stable steady-state radius corresponding to the increased ambient pressure.

The same qualitative picture applies also to the change in oscillation frequency of shape modes owing to the step change in shape for a non-zero coefficient A_n. For positive A_n, the bubble is deformed into an oblate shape, and the frequency of shape oscillations is increased, whereas for negative A_n, the bubble is prolate and the frequency of oscillation is decreased. In this case, it is known from prior studies

(Kang & Leal 1990) of bubble oscillation in a uniaxial flow that the frequency decreases as the degree of deformation increases in the prolate case ($A_n < 0$), and becomes equal to zero at the critical deformation beyond which steady solutions for the bubble shape cease to exist. An asymptotic prediction for the critical value of A_n can also be obtained from (4.37). For a bubble in a biaxial flow, on the other hand, prior studies show that steady solutions for the bubble shape exist to high degrees of deformation (high Weber number) and there is no indication of the same type of limit point behaviour that was observed for prolate shapes. It is thus not surprising that the frequency of oscillation actually increases in this case for increasing A_n.

It should be noted that the modification in oscillation frequency is present for all conditions, including the two limits of resonant interactions between shape and volume modes. However, as we shall see in the next sub-section, we may expect the frequency shift to be modified somewhat in the resonant case compared to non-resonant case.

4.2.1. *Resonant interaction at* $\omega_0 = \omega_n$

Let us now consider the nature of the resonance for $\omega_0 = \omega_n$. In this case, the conditions for the absence of secular terms in (4.31) and (4.32) are

$$\frac{\mathrm{d}\alpha_{1,0}}{\mathrm{d}\tau} = -\mathrm{i}H_1\alpha_{1,n} + \mathrm{i}H_2\alpha_{1,0}, \tag{4.39}$$

$$\frac{\mathrm{d}\alpha_{1,n}}{\mathrm{d}\tau} = -\mathrm{i}H_3\alpha_{1,0} + \mathrm{i}H_4\alpha_{1,n}, \tag{4.40}$$

where
$$H_1 = \frac{(n-3)A_n}{2(2n+1)\omega_0}, \quad H_3 = \frac{(n+1)(n-3)A_n}{2\omega_n}. \tag{4.41}$$

As noted above, (4.39) and (4.40) still retain the self-induced resonance terms with coefficients H_2 and H_4 that were defined in (4.35), and, in addition, contain new terms proportional to H_1 and H_3 that correspond to resonance interactions between modes. Thus, in the resonant case, it is necessary to determine $\alpha_{1,0}$ and $\alpha_{1,n}$ so as to simultaneously eliminate both types of secular terms. This means that the frequency shift associated with H_2 and H_4 will be modified somewhat relative to the case with no resonance. Furthermore, the presence of a frequency shift away from the fundamental frequencies ω_0 and ω_n means that the dynamic response due to mode–mode interactions should correspond to a slight detuning away from exact resonance.

Since (4.39) and (4.40) are linear, we can proceed formally toward an analytic solution. For this purpose, it is convenient to express $\alpha_{1,0}$ and $\alpha_{1,n}$ in the form,

$$\alpha_{1,0} = x_0 + \mathrm{i}y_0, \quad \alpha_{1,n} = x_n + \mathrm{i}y_n, \tag{4.42}$$

and then write (4.39) and (4.40) as a first-order dynamical system

$$\dot{\boldsymbol{x}} = \boldsymbol{A}\cdot\boldsymbol{x}, \tag{4.43}$$

where
$$\boldsymbol{x} = (x_0, y_0, x_n, y_n)^{\mathrm{T}}, \tag{4.44a}$$

and
$$\boldsymbol{A} = \begin{bmatrix} 0 & -H_2 & 0 & H_1 \\ H_2 & 0 & -H_1 & 0 \\ 0 & H_3 & 0 & -H_4 \\ -H_3 & 0 & H_4 & 0 \end{bmatrix}. \tag{4.44b}$$

It is well-known that the solution of (4.43) can then be expressed in the exponential operator form

$$\boldsymbol{x} = \mathrm{e}^{\boldsymbol{A}t} \cdot \boldsymbol{x}_0, \tag{4.45}$$

where $$\boldsymbol{x}_0 = \boldsymbol{x}(t=0) = \left(\frac{A_0}{\omega_0^2}, 0, \frac{(n+1)A_n}{\omega_n^2}, 0\right)^{\mathrm{T}}$$

The qualitative nature of the solution (4.45) is completely determined by the eigenvalues of the matrix $\boldsymbol{A}$, which are the roots of the equation

$$\lambda^4 + (2H_1H_3 + H_2^2 + H_4^2)\lambda^2 + (H_1H_3 - H_2H_4)^2 = 0. \tag{4.46}$$

Since $$2H_1H_3 + H_2^2 + H_4^2 > 0,$$

(recall that $H_1H_3 > 0$), and the discriminant is also positive, i.e.

$$(2H_1H_3 + H_2^2 + H_4^2)^2 - 4(H_1H_3 - H_2H_4)^2 = [4H_1H_3 + (H_2 - H_4)^2](H_2 + H_4)^2 > 0,$$

the four roots of (4.46) must be pure imaginary. Indeed, it can be shown after a little algebra that the four eigenvalues of $\boldsymbol{A}$ are

$$\lambda = \pm \mathrm{i}\Omega_1, \pm \mathrm{i}\Omega_2, \tag{4.47}$$

where $$\Omega_{1,2} = \tfrac{1}{2}((4H_1H_3 + (H_2 - H_4)^2)^{\frac{1}{2}} \pm |H_2 + H_4|). \tag{4.48}$$

It follows that the components of $\boldsymbol{x}$ are all linear combinations of sinusoidal functions of $\Omega_1\tau$ and $\Omega_2\tau$. Hence, knowing $x_0(\tau)$, $y_0(\tau)$, $x_n(\tau)$ and $y_n(\tau)$, we can easily understand the dynamics associated with (4.39) and (4.40). We can write

$$\alpha_{1,0} = M_0 \exp(\mathrm{i}\Theta_0), \quad \alpha_{1,n} = M_n \exp(\mathrm{i}\Theta_n), \tag{4.49}$$

where $$M_0 = (x_0^2 + y_0^2)^{\frac{1}{2}}, \quad M_n = (x_n^2 + y_n^2)^{\frac{1}{2}},$$

and $$\Theta_0 = \tan^{-1}\frac{y_0}{x_0}, \quad \Theta_n = \tan^{-1}\frac{y_n}{x_n}.$$

It follows that the generic behaviour in this case is that both the breathing mode and the P_n mode undergo continuous oscillations at $O(\epsilon)$. This is fundamentally different from the behaviour following a pressure impulse, or from the oscillations following an initial perturbation in shape (Longuet-Higgins). In these cases, the dynamics reduced to a one-way transfer of energy from the deformation mode to the breathing mode. Here, the two modes continuously exchange energy on the slow time-scale, $\tau \sim O(1)$, and thus, in a non-dissipative system, they both remain $O(\epsilon)$ for all times.

The exception to this generic behaviour occurs when A_n, and thus M_n, is zero at $t = 0$. In the polar representation (4.49), the governing equations (4.39) and (4.40) can be expressed in the alternative form

$$\frac{\mathrm{d}M_0}{\mathrm{d}\tau} = H_1M_n \sin(\Theta_n - \Theta_0), \quad \frac{\mathrm{d}M_n}{\mathrm{d}\tau} = -H_3M_0 \sin(\Theta_n - \Theta_0), \tag{4.50}$$

$$M_0\frac{\mathrm{d}\Theta_0}{\mathrm{d}\tau} = H_2M_0 - H_1M_n\cos(\Theta_n - \Theta_0), \quad M_n\frac{\mathrm{d}\Theta_n}{\mathrm{d}\tau} = H_4M_n - H_3M_0\cos(\Theta_n - \Theta_0), \tag{4.51}$$

with initial conditions

$$M_0(0) = \frac{A_0}{\omega_0^2}, \quad M_n(0) = \frac{(n+1)A_n}{\omega_n^2}, \quad \Theta_0(0) = \Theta_n(0) = 0. \tag{4.52}$$

Eliminating $\sin(\Theta_n - \Theta_0)$ from (4.50), it can be shown that

$$H_3 M_0^2(\tau) + H_1 M_n^2(\tau) = \text{constant}, \tag{4.53}$$

which represents a surface energy conservation equation for the bubble oscillation. Now, if $M_n = A_n = 0$ at $\tau = 0$, we see from the definition (4.41) that

$$H_1 = H_3 = 0 \quad \text{at } \tau = 0,$$

and thus,

$$\frac{\mathrm{d}M_0}{\mathrm{d}\tau} = \frac{\mathrm{d}M_n}{\mathrm{d}\tau} = 0,$$

while

$$\frac{\mathrm{d}\Theta_0}{\mathrm{d}\tau} = H_2.$$

It follows that M_n remains zero for all time, and thus M_0 is also constant at its initial value. Θ_0, on the other hand, increases linearly with t, and this corresponds to the frequency shift in the radial mode that occurs because the step change in pressure induces a change in the bubble volume. The fact that $M_n = 0$ simply means that there is no resonant mode-coupling for a bubble that initially undergoes only a volume change, and in this case the deformation mode remains at zero. The result $M_0 = \text{const.} \neq 0$ means that the bubble oscillates only on the timescale, $t = O(1)$, with a modified frequency, but without any slow oscillation in amplitude as occurs for other initial conditions.

In order to further illustrate the predicted behaviour for this $1-1$ resonance case (i.e. $\omega_0 = \omega_n$), we have integrated (4.50) and (4.51) numerically for $n = 4$, and three sets of initial values for M_0 and M_4. The results are shown in figure 4. The first case, for a very small initial value of $M_4 = 0.05$ and $M_0 = 1$, is similar in behaviour to the limit $M_4(0) = 0$. The increase of both Θ_0 and Θ_n is approximately linear in τ. Thus both the radial and P_4 modes oscillate at an increased frequency owing to the change in bubble volume, but the effect on the radial mode is clearly larger. The second case is for $M_0(0) = 0.9$ and $M_4(0) = 1.1$. In this case, the amplitudes of both modes oscillate on the long timescale $\tau = O(1)$, though the amplitude of the shape oscillation is very much larger. This may be slightly misleading, however, if our interest is with the relative contributions of the $n = 0$ and $n = 4$ modes to the bubble volume. The volume oscillation associated with M_0 is 0 (ϵM_0). On the other hand, the volume oscillation due to the oscillations of shape is much smaller, only $O(\epsilon^2 M_n^2)$. Finally, the last case considered is $M_0(0) = 0.05$ and $M_n(0) = 1$. In this case, there is a significant coupling between modes which leads to moderate fluctuations in M_0 via energy exchange with the larger oscillations of the bubble shape. It may be noted that all three of the cases shown in figure 4 that the phase functions $\Theta_0(\tau)/\tau$ and $\Theta_4(\tau)/\tau$ are very weak functions of t and thus that $\Theta_0(\tau)$ and $\Theta_4(\tau)$ are nearly linear in τ. This implies that the phase modulation corresponds very nearly to a simple frequency shift. Based upon the numerical results in figure 4(*b*) for the case $M_0(0) = 0.9$ and $M_4(0) = 1.1$, we can easily estimate the modified frequencies for the two modes of oscillation to be

$$\Omega_0 = \omega_0(1 + 2.11\epsilon), \quad \Omega_4 = \omega_4(1 + 1.58\epsilon). \tag{4.54}$$

4.2.2. *Resonant interaction at* $\omega_0 = 2\omega_n$

The second case of resonant interactions following a step change in the pressure distribution at the bubble surface occurs when $\omega_0 = 2\omega_n$. In this case, the condition to exclude secular terms in (4.31) and (4.32) is

$$\frac{\mathrm{d}\alpha_{1,0}}{\mathrm{d}\tau} = \mathrm{i}H_5 \alpha_{1,0}^2 + \mathrm{i}H_2 \alpha_{1,0}, \quad \frac{\mathrm{d}\alpha_{1,n}}{\mathrm{d}\tau} = \mathrm{i}H_6 \alpha_{1,0} \alpha_{1,n}^* + \mathrm{i}H_4 \alpha_{1,n}. \tag{4.55}$$

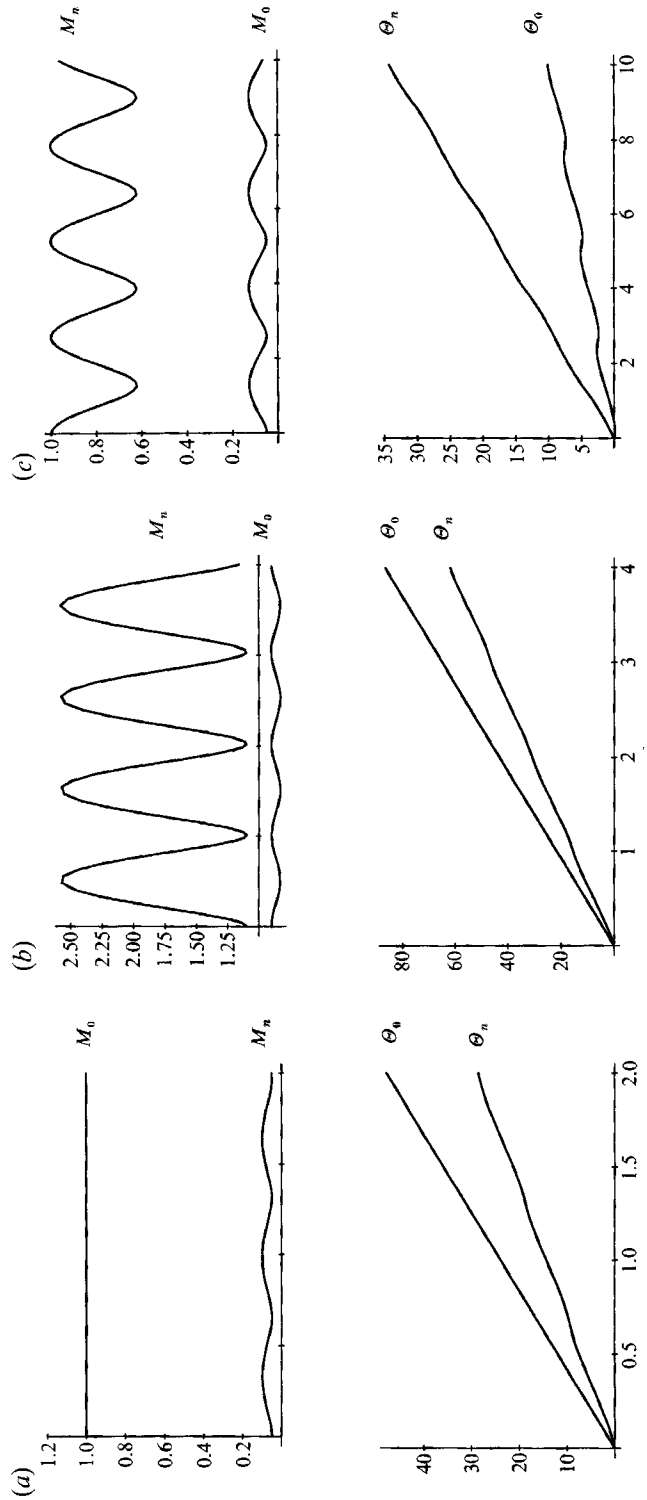

FIGURE 4. The amplitude functions and phase angles as a function of the slow timescale τ, at the resonant state $\omega_0 = \omega_4$. (*a*) $M_4(0) - 0.05$, $M_0(0) = 1.0$; (*b*) $M_4(0) - 1.1$, $M_0(0) = 0.9$; (*c*) $M_4(0) - 1.0$, $M_0(0) - 0.05$.

The coefficients H_5 and H_6 were defined earlier in conjunction with (4.14) and (4.15), while H_2 and H_4 are defined in (4.35). Clearly, these equations resemble (4.14) and (4.15), but now include the self-induced secular terms involving H_2 and H_4 that correspond to a frequency shift, and thus a 'detuning' of the primary resonant interactions. As shown in the preceding section, such detuning will tend to produce a continuous exchange between the radial and shape deformation modes, rather than the one-way energy transfer that was found for the case of a pressure impulse under the same conditions, $\omega_0 = 2\omega_n$.

By applying the type of polar decomposition defined in (4.16), we can obtain a system of four differential equations governing the amplitude and frequency modulations for the bubble oscillation

$$\frac{\mathrm{d}M_0}{\mathrm{d}\tau} = -H_5 M_n^2 \sin(2\Theta_n - \Theta_0), \quad \frac{\mathrm{d}M_n}{\mathrm{d}\tau} = H_6 M_0 M_n \sin(2\Theta_n - \Theta_0), \tag{4.56}$$

$$M_0 \frac{\mathrm{d}\Theta_0}{\mathrm{d}\tau} = H_2 M_0 + H_5 M_n^2 \cos(2\Theta_n - \Theta_0), \quad \frac{\mathrm{d}\Theta_n}{\mathrm{d}\tau} = H_4 + H_6 M_0 \cos(2\Theta_n - \Theta_0), \tag{4.57}$$

with the same initial condition as in the previous case $\omega_0 = \omega_n$. In this case, the energy equation for the oscillation can be derived from (4.56). The result is

$$H_6 M_0^2(\tau) + H_5 M_n^2(\tau) = \text{constant} \quad (\tau \geqslant 0). \tag{4.58}$$

For general cases, in which $A_n \neq 0$, the nonlinear differential equations (4.56) and (4.57) can only be solved numerically. However, in the special case where $A_n = 0$, $A_0 \neq 0$, it can be seen that $\mathrm{d}M_n/\mathrm{d}\tau = 0$, $\mathrm{d}M_0/\mathrm{d}\tau = 0$ at $\tau = 0$, and thus $M_n = 0$, $M_0 = A_0/\omega_0^2$ for all τ. Further, $\mathrm{d}\Theta_0/\mathrm{d}\tau = H_2$ so that $\Theta_0 = H_2\tau$. Thus, if we begin with a step change in only the isotropic contribution to the pressure on the bubble surface, the response is simply radial oscillations with a modified frequency, $\omega_0 = \epsilon H_2$, which is either increased or decreased depending upon whether A_0 (and thus H_2) is positive or negative. There is no coupling in this case with the shape deformation mode of oscillation.

On the other hand, we can show via numerical analysis that resonant coupling exists when $A_n \neq 0$, for arbitrary A_0. A typical case is shown in figure 5 for $\omega_0 = 2\omega_4$, and $M_0(0) = 0.9$ and $M_4(0) = 1.1$. It can be seen from figure 5(*a*) that the two resonant modes exchange energy continuously and sustain oscillations at all times. However, even if $A_0 = 0$, there is a transfer of energy from the deformation mode to the radial mode, and this is again followed by a continuous exchange of energy between the two modes at $O(\epsilon)$. The sustained energy exchange for these cases is essentially due to the frequency detuning that results from the change in the steady-state bubble radius and shape at $O(\epsilon)$ induced by the step change in pressure (i.e. $A_0 \neq 0, A_n \neq 0$). It is also noteworthy that the amount of energy exchange at $\omega_0 = 2\omega_n$ is much larger than that which occurs for resonance at $\omega_0 = \omega_n$ with (approximately) the same set of initial conditions (compare figures 4(*b*) and 5). As in the previous case $\omega_0 = \omega_n$, the change in the steady-state bubble radius and shape at $O(\epsilon)$ due to the step change in the average ambient pressure (i.e. $A_0 \neq 0, An_0 \neq 0$) leads to a phase modulation in each mode, which is monotonically increased with τ (see figure 4*b*).

It can be noted from (4.56) and (4.57) that the phase modulation for each mode is very sensitive to the sign of A_0 (i.e. $M_0(0)$). When $A_0 > 0$, the phase modulation for each mode increases with τ, and vice versa. As in the previous case ($\omega_0 = \omega_n$), $\Theta_0(\tau)/\tau$ and $\Theta_n(\tau)/\tau$ are very weak functions of τ. When $n = 4$, $M_0(0) = 0.9$ and $M_4(0) = 1.1$,

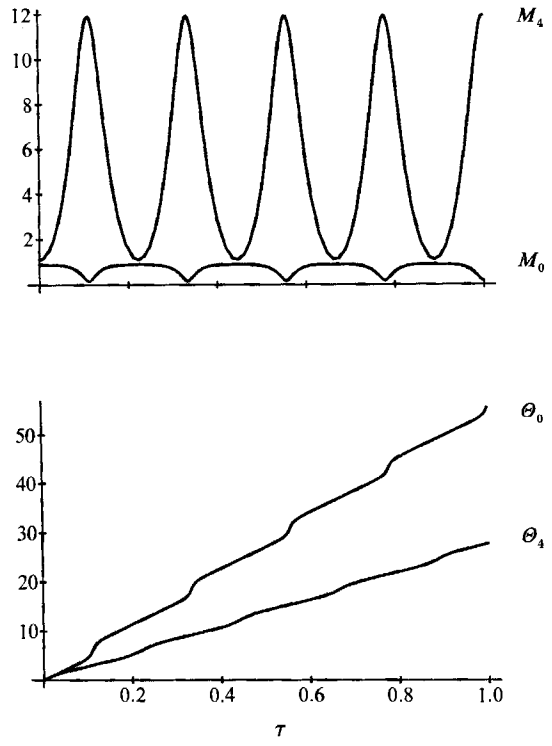

FIGURE 5. Amplitude modulations $M_0(\tau)$ and $M_4(\tau)$ and phase angles versus the slow timescale τ at the resonant state $\omega_0 = 2\omega_4$: $M_0(0) = 0.9$, $M_4(0) = 1.1$ and $\gamma = 1$.

it is found that $\Theta_0(\tau) \sim 2.74\omega_0\tau$ and $\Theta_4(\tau) \sim 2.95\omega_4\tau$. Then, the frequency of each oscillation is

$$\Omega_0 = \omega_0(1+2.74\epsilon), \quad \Omega_4 = \omega_4(1+2.95\epsilon), \tag{4.59}$$

whereas the modified frequency for $M_0(0) = \pm 1$ and $M_4(0) = 0$ is determined from (4.37) to be

$$\Omega_0 = \omega_0(1 \pm 2.5\epsilon). \tag{4.60}$$

Comparing (4.54) and (4.59), it can be seen that the bubble oscillation at $\omega_0 = 2\omega_n$ in the presence of a non-uniform pressure distribution becomes much more unstable than it would be at $\omega_0 = \omega_n$. This is a consequence of the increased amount of energy exchange between the two resonant modes at $\omega_0 = 2\omega_n$ relative to the case $\omega_0 = \omega_n$.

In figure 6, the phase trajectories, $M_4(\tau)$ vs. $M_0(\tau)$, are plotted for various sets of initial conditions (i.e. A_0 and A_n). The present phase trajectories at the resonance condition $\omega_0 = 2\omega_n$ induced by a step change in the pressure are qualitatively different from those obtained for the resonance at $\omega_0 = 2\omega_n$ induced by an impulse in the pressure. In the present case, the two resonant modes exchange energy continuously and sustain oscillations at all times unless either $A_0 = 0$ or $A_n = 0$. It is worth pointing out that in the step response, the bubble oscillates around the 'new' steady-state shape which is non-spherical owing to the non-uniform pressure distribution ($A_n \neq 0$). In addition, the bubble radius (or volume) is changed at $O(\epsilon)$ from the initial equilibrium value owing to the reduced (or increased) average pressure ($A_0 \neq 0$). We may anticipate that these two combined effects can also be produced by imposition of an external mean flow, which we shall consider in §5.

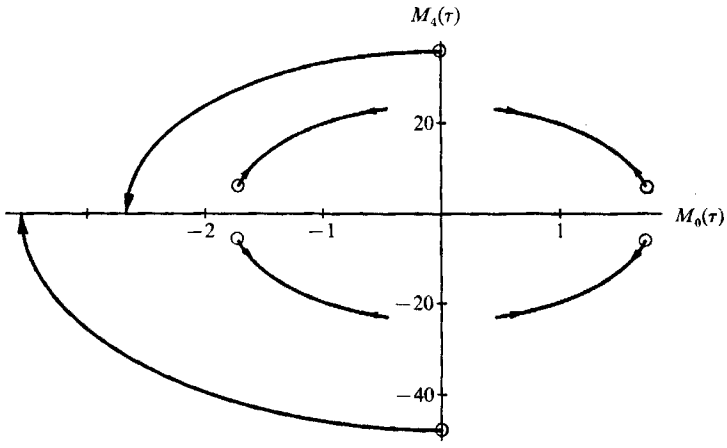

FIGURE 6. Phase diagram $M_4(\tau)$ *vs.* $M_0(\tau)$, for various sets of initial conditions $\{M_0(0), M_4(0)\}$: ○, initial points of the phase trajectories.

5. Bubble oscillation in a uniaxial straining flow

In this section, we generalize our investigation of the dynamic response of an ideal gas bubble to include the influence of steady deformation due to interaction with a steady mean flow. Specifically, we consider a bubble with the steady-state shape, (3.5), due to a uniaxial straining flow, when the (acoustic radiation) pressure at the bubble surface undergoes an abrupt, but asymptotically small change, (4.2) or (4.26), at some initial instant.

We begin with the response to an impulsive change in pressure. In this case, it can be anticipated from the previous section, that the frequency of oscillation of both the radial and shape deformation modes will decrease with increase of the steady deformation, and this is again reflected in the present analysis by the appearance of (self-induced) secular terms beginning at $O(\epsilon^2)$.

The presence of the external flow produces qualitatively new effects when we consider mode–mode interactions. One new feature is that the leading-order correction to the bubble volume occurs at $O(\epsilon^{\frac{3}{2}})$, rather than $O(\epsilon^2)$ as in the previous examples, and this new 'breathing' mode of oscillation can exhibit resonant interactions with the P_2 mode of shape oscillation in the special case $\omega_0 = \omega_2$, to produce changes in the oscillation amplitudes at $O(\epsilon)$ on the intermediate timescale $\epsilon^{\frac{1}{2}}t$.

In addition, at $O(\epsilon^2)$, three distinct kinds of secular terms are possible. The first is the self-induced effect, described earlier, which is always present when the bubble is deformed, and leads to a decrease in oscillation frequency with increase in the degree of bubble deformation in the steady flow. The second occurs when $\omega_0 = 2\omega_n$ and corresponds to a resonant interaction between the breathing and shape modes of oscillation that influences the amplitude of oscillation at $O(\epsilon)$ on the slow timescale ϵt. Although an apparently similar resonance was found in the previous section in the *absence* of any mean flow, we shall see that the existence of a non-spherical steady-state shape leads to new effects in the nature of the slow timescale variations of the interacting modes. Finally, resonant interactions between the breathing and deformation modes appear when $\omega_0 = \omega_n$, but in this case this is solely a consequence of the presence of the mean flow – i.e. this type of 1–1 resonance did not appear with an initial pressure *impulse* in the absence of flow.

We begin by outlining the governing equations, and their solutions through terms of $O(\epsilon^2)$, in the generic case where mode–mode resonant interactions do not occur (i.e. $\omega_0 \neq \omega_n, \omega_0 \neq 2\omega_n$). In this case, the only secular terms in the analysis appear beginning at $O(\epsilon^2)$, owing to the changes of frequency in the $O(\epsilon)$ shape and volume oscillations that are caused by bubble deformation in the steady flow. [It should be noted that such frequency shifts due to steady deformation are also expected to occur in the shape and volume oscillations, at $O(\epsilon^{\frac{3}{2}})$ and $O(\epsilon^2)$. However, in the present solution scheme, these would only be reflected by the appearance of 'self-induced' secular terms in the dynamical equations at $O(\epsilon^{\frac{5}{2}})$ and $O(\epsilon^3)$, and we do not calculate any solutions at this level of approximation.]

After we have considered this generic case, in which resonant interactions between modes are not present, we turn to the special resonant cases when $\omega_0 = \omega_n$ and $\omega_0 = 2\omega_n$.

5.1. *Bubble oscillation in the absence of mode–mode resonant interactions*

We begin, as stated above, by considering the case of an $O(\epsilon)$ impulsive change of pressure when ω_0 does not take either of the special values $\omega_n\,(n \geqslant 2)$ or $2\omega_n\,(n \geqslant 2)$. In general, our analysis follows the asymptotic expansion scheme (2.13) and (2.14). However, since we anticipate the likelihood of secular behaviour at $O(\epsilon^{\frac{3}{2}})$ and $O(\epsilon^2)$, for the special conditions $\omega_0 = \omega_n$ or $\omega_0 = 2\omega_n$, it is convenient to formulate the governing equations right from the beginning in a form suitable for a multiple-timescale solution procedure. In this framework, the bubble shape functions f_j at each order in $\epsilon^{\frac{1}{2}}$, and the corresponding velocity potential functions ϕ_j are considered to be functions not only of t, as in (2.15) and (2.16)–(2.17), but also of two slowly varying timescales, $\epsilon^{\frac{1}{2}}t$ and ϵt, all considered as independent variables, i.e.

$$f_j = \sum_{n=0}^{\infty} a_{j,n}(t, \zeta, \tau)\, P_n(\eta), \tag{5.1}$$

$$\phi_j = \sum_{n=0}^{\infty} b_{j,n}(t, \zeta, \tau) \frac{P_n(\eta)}{r^{n+1}}, \tag{5.2}$$

where

$$\zeta \equiv \epsilon^{\frac{1}{2}}t, \quad \tau \equiv \epsilon t. \tag{5.3}$$

At the leading order, $O(\epsilon)$, the amplitude functions $a_{1,n}$ and $b_{1,n}$, take the same form (4.11) and (4.12), as in the case without a mean flow, i.e.

$$a_{1,n}(t, \zeta, \tau) = \tfrac{1}{2}\{\alpha_{1,n}(\zeta, \tau) \exp(\mathrm{i}\omega_n t) + a^{\mathrm{s}}_{1,n}\} + \text{c.c.}, \tag{5.4}$$

$$b_{1,n}(t, \zeta, \tau) = -\frac{\mathrm{i}\omega_n}{2(n+1)} \alpha_{1,n}(\zeta, \tau) \exp(\mathrm{i}\omega_n t) + \text{c.c.}, \tag{5.5}$$

with

$$\alpha_{1,n}(0, 0) = \frac{A_n(n+1)\,\mathrm{i}}{\omega_n}. \tag{5.6}$$

As usual, the slowly varying functions $\alpha_{1,n}$ will be chosen in such a way as to eliminate any secular terms that appear in the governing equations at $O(\epsilon^{\frac{3}{2}})$ or $O(\epsilon^2)$.

In the presence of the mean flow, $\epsilon^{\frac{1}{2}}\phi_0^{\mathrm{s}}$ given by (3.1), the second term in the expansion for f and ϕ occurs at $O(\epsilon^{\frac{3}{2}})$. Governing equations for the radial, P_2 and P_4 modes of oscillation at $O(\epsilon^{\frac{3}{2}})$, can be obtained from the general equations (2.8) and (2.11) and the forms of the $O(\epsilon)$ solutions above.

5.1.1. $O(\epsilon^{\frac{3}{2}})$ *problem*

Radial mode

$$\frac{\partial^2}{\partial t^2} a_{2,0} + \omega_0^2 a_{2,0} = -\mathrm{i}\omega_0 \frac{\partial \alpha_{1,0}}{\partial \zeta} \exp(\mathrm{i}\omega_0 t) - \tfrac{1}{6}\mathrm{i}\omega_2 \alpha_{1,2} \exp(\mathrm{i}\omega_2 t) + \text{c.c.} \tag{5.7}$$

P_2 *mode*

$$\frac{\partial^2}{\partial t^2} a_{2,2} + \omega_2^2 a_{2,2} = -\mathrm{i}\omega_2 \frac{\partial \alpha_{1,2}}{\partial \zeta} \exp(\mathrm{i}\omega_2 t) + \tfrac{5}{2}\mathrm{i}\omega_0 \alpha_{1,0} \exp(\mathrm{i}\omega_0 t) - \tfrac{25}{21}\mathrm{i}\omega_4 \alpha_{1,4} \exp(\mathrm{i}\omega_4 t) + \text{c.c.} \tag{5.8}$$

P_4 *mode*

$$\frac{\partial^2}{\partial t^2} a_{2,4} + \omega_4^2 a_{2,4} = -\mathrm{i}\omega_4 \frac{\partial \alpha_{1,4}}{\partial \zeta} \exp(\mathrm{i}\omega_4 t) + \tfrac{25}{7}\mathrm{i}\omega_2 \alpha_{1,2} \exp(\mathrm{i}\omega_2 t) + \text{c.c.} \tag{5.9}$$

Governing equations for the higher order $P_n\,(n > 4)$ deformation modes can be obtained in the same manner.

It is clear from the forms of the right-hand sides of (5.7)–(5.9), that there are no resonant effects at $O(\epsilon^{\frac{3}{2}})$ unless $\omega_0 = \omega_2$. Hence, apart from the exceptional case when $\omega_0 = \omega_2$, it is clear that

$$\frac{\partial}{\partial \zeta} \alpha_{1,n} = 0 \tag{5.10}$$

for all n, and thus $\alpha_{1,n}$ is at most a function of the slower time variable τ. The $O(\epsilon^{\frac{3}{2}})$ solution thus takes the general form

$$a_{2,0} = \frac{1}{2(\omega_2^2 - \omega_0^2)} \{A_2 \exp(\mathrm{i}\omega_0 t) + \tfrac{1}{3}\mathrm{i}\omega_2 \alpha_{1,2}(\tau) \exp(\mathrm{i}\omega_2 t)\} + \text{c.c.} \tag{5.11}$$

$$a_{2,2} = \frac{5}{2(\omega_2^2 - \omega_0^2)} \{A_0 \exp(\mathrm{i}\omega_2 t) + \mathrm{i}\omega_0 \alpha_{1,0}(\tau) \exp(\mathrm{i}\omega_0 t)\} + \frac{125}{21(\omega_4^2 - \omega_2^2)} \{A_4 \exp(\mathrm{i}\omega_2 t) + \tfrac{1}{5}\mathrm{i}\omega_4 \alpha_{1,4}(\tau) \exp(\mathrm{i}\omega_4 t)\} + \text{c.c.} \tag{5.12}$$

$$a_{2,4} = \frac{75}{7(\omega_4^2 - \omega_2^2)} \{A_2 \exp(\mathrm{i}\omega_4 t) + \tfrac{1}{3}\mathrm{i}\omega_2 \alpha_{1,2}(\tau) \exp(\mathrm{i}\omega_2 t)\} + \text{c.c.} \tag{5.13}$$

It is evident that these solutions for $a_{2,0}$ and $a_{2,2}$ are not valid when $\omega_0 = \omega_2$ owing to the existence of a resonant interaction between the radial and P_2-modes. We shall consider this special case shortly.

The significance of the solutions (5.11)–(5.13) at $O(\epsilon^{\frac{3}{2}})$ is twofold. First, the strength of mode–mode interactions is strongly enhanced owing to the presence of a mean flow which deforms the bubble, compared to the interactions in the absence of flow which only occur at $O(\epsilon^2)$. This means, for example, that a radial oscillation is induced at $O(\epsilon^{\frac{3}{2}})$ owing to a perturbation in the initial shape, whereas in the absence of flow it could only be $O(\epsilon^2)$ (in the non-resonant case). Of course, it cannot be concluded that the magnitude of volume or shape oscillations due to interactions with a mean flow will always be $O(\epsilon^{\frac{3}{2}})$ in a small-amplitude expansion. This is a consequence of the specific choice of an undisturbed flow of $O(\epsilon^{\frac{1}{2}})$ which induces steady deformation at $O(\epsilon)$, coupled with a pressure perturbation of $O(\epsilon)$. However, the general conclusion

of enhanced mode–mode coupling due to flow will most certainly carry over to other cases.

The second point of significance of the solutions (5.11)–(5.13), is that the nature of modal coupling is fundamentally different from that in cases examined previously without flow. Specifically, the existence of a radial mode contribution at $O(\epsilon^{\frac{3}{2}})$ is solely due to interactions between the mean flow and the initial P_2 mode of deformation – there is no dependence of $a_{2,0}$ on A_0. Similarly, the P_2 contribution at $O(\epsilon^{\frac{5}{2}})$ is dependent on A_0 and A_4, but not A_2, and so on. One very important implication of this is that a mechanism now exists to generate a time-dependent shape oscillation even when the initial condition involves only an impulse in volume (i.e. $A_0 \neq 0, A_n = 0$). In all cases without flow, coupling between shape and volume modes was only possible if $A_n \neq 0$. If $A_0 \neq 0$ but $A_n = 0$, we previously found that the bubble only oscillated radially for all times. The mechanism for generation of a shape oscillation in this case is simply that the change of bubble radius causes the surface stresses associated with the mean flow to become time-dependent owing to the time-dependent position of the bubble surface.

Before studying the resonant interactions at $O(\epsilon^{\frac{3}{2}})$, let us complete our investigation of the generic case where $\omega_0 \neq \omega_n$ or $\omega_0 \neq 2\omega_n$, by considering the $O(\epsilon^2)$ terms in the expansion. The governing equations at $O(\epsilon^2)$ are again obtained from the general equations (2.8) and (2.11), and now depend on the forms of the solutions for both $a_{1,n}$ and $a_{2,n}$. For brevity, we show explicitly, only the equations for $a_{3,0}$, $a_{3,2}$ and $a_{3,4}$.

5.1.2. $O(\epsilon^2)$ *problem*

Radial mode

$$\frac{\partial^2}{\partial t^2}a_{3,0}+\omega_0^2 a_{3,0} = \left[-\mathrm{i}\omega_0\frac{\partial}{\partial\tau}\alpha_{1,0}+\left\{\frac{5\omega_2^2}{6(\omega_2^2-\omega_0^2)}+\frac{3\gamma\omega_0^2+2(3\gamma-1)}{2}a_{1,0}^{\mathrm{s}}\right\}\alpha_{1,0}\right]\exp(\mathrm{i}\omega_0 t)$$
$$+\left[\frac{90-5\omega_0^2}{336}\alpha_{1,2}-\mathrm{i}\omega_2\left\{\frac{5A_0}{\omega_2^2-\omega_0^2}+\frac{125A_4}{819}\right\}\right]\exp(\mathrm{i}\omega_2 t)$$
$$-\frac{685}{1638}\alpha_{1,4}\exp(\mathrm{i}\omega_4 t)+\sum_{n=2}\frac{\alpha_{1,n}^2}{8(2n+1)}\left\{\frac{4n+9}{n+1}\omega_n^2-2\omega_0^2\right\}\exp(2\mathrm{i}\omega_n t)$$
$$+\text{c.c.}+\text{non-secular terms.} \tag{5.14}$$

P_2-mode

$$\frac{\partial^2}{\partial t^2}a_{3,2}+\omega_2^2 a_{3,2} = \left[-\mathrm{i}\omega_2\frac{\partial}{\partial\tau}\alpha_{1,2}+\left\{\frac{3040}{819}+\frac{5(7\omega_0^2-36)}{2\omega_0^2(\omega_0^2-\omega_2^2)}\right\}\alpha_{1,2}\right]\exp(\mathrm{i}\omega_2 t)$$
$$+\left[\frac{1200-25\omega_0^2}{672}\alpha_{1,0}+\frac{5\mathrm{i}\omega_0 A_2}{2(\omega_2^2-\omega_0^2)}\right]\exp(\mathrm{i}\omega_0 t)$$
$$-21\alpha_{1,0}\alpha_{1,2}^*\exp(\mathrm{i}(\omega_0-\omega_2)t)$$
$$+\text{c.c.}+\text{non-secular-terms.} \tag{5.15}$$

P_4-mode

$$\frac{\partial^2}{\partial t^2}a_{3,4}+\omega_4^2 a_{3,4} = \left[-\mathrm{i}\omega_4\frac{\partial}{\partial\tau}\alpha_{1,4}+\frac{25}{4}\left\{\frac{34649}{48279}+\frac{9}{\omega_0^2}\right\}\alpha_{1,4}\right]\exp(\mathrm{i}\omega_4 t)$$
$$+\frac{3175}{182}\alpha_{1,0}\exp(\mathrm{i}\omega_0 t)-\frac{675}{2}\alpha_{1,4}^*\exp[\mathrm{i}(\omega_0-\omega_4)t]$$
$$+\text{c.c.}+\text{non-secular terms.} \tag{5.16}$$

As noted earlier, there are three possible secular terms in these $O(\epsilon^2)$ equations. Two result from resonant interactions between the radial and shape deformation modes, when either $\omega_0 = \omega_n$ or $\omega_0 = 2\omega_n$. We shall discuss these special cases (which also includes $\omega_0 = \omega_2$) later in this section. However, even when $\omega_0 \neq \omega_n$ or $\omega_0 \neq 2\omega_n$, the governing equations (5.14)–(5.16) still contain secular terms, which must be eliminated if the solutions for $a_{3,n}$ are to remain bounded. These are the so-called 'self-induced' secular terms that appeared earlier in the analysis of a step change in pressure without the mean flow. We have already seen in §4, that they correspond to a decrease in the frequency of oscillation of the $O(\epsilon)$ solution with increased steady deformation of the bubble, rather than a change in the amplitude of oscillation as occurs in cases with mode–mode resonant interactions.

To obtain bounded solutions at $O(\epsilon^2)$ for this non-resonant case, the slowly varying coefficients in the $O(\epsilon)$ solutions must be chosen to eliminate the 'self-induced' secular terms in (5.14)–(5.16). It can be shown very simply that the resulting solutions for these coefficient functions can be expressed in the form

$$\alpha_{1,n}(\tau) = \frac{A_n(n+1)\,\mathrm{i}}{\omega_n}\exp(-\mathrm{i}\,Q_n\tau), \tag{5.17}$$

where

$$Q_0 = \frac{15\gamma\omega_0^4 - 50(3\gamma+5)\,\omega_0^2 - 120(3\gamma-1)}{24\omega_0^4(\omega_0^2-\omega_2^2)},$$

$$Q_2 = \frac{760}{2457} + \frac{5(7\omega_0^2-36)}{24\omega_0^2(\omega_0^2-\omega_2^2)},$$

$$Q_4 = \frac{5}{24}\left(\frac{34649}{144837} + \frac{3}{\omega_0^2}\right),$$

and so on for larger values of n. Combining (5.4) and (5.17), it follows that the complete solutions for the bubble response at $O(\epsilon)$ can be expressed in the form

$$a_{1,n}(t) = a_{1,n}^{\mathrm{S}} - \frac{A_n(n+1)}{\omega_n}\sin\{\omega_n(1-Q_n\,\epsilon)\,t\}, \tag{5.18}$$

$$\phi_{1,n}(t,r,n) = A_n\cos\{\omega_n(1-Q_n\,\epsilon)\,t\}\frac{P_n(\eta)}{r^{n+1}}, \tag{5.19}$$

assuming only that $\omega_0 \neq \omega_n$ or $\omega_0 \neq 2\omega_n$. The fact that the $O(\epsilon^{\frac{3}{2}})$ solutions (5.11)–(5.13) break down when $\omega_0 = \omega_2$ is clearly reflected in the forms for Q_0 and Q_2.

As anticipated, the self-induced secularity at $O(\epsilon^2)$ generates only a modification in the frequency of each mode (provided $\omega_0 \neq \omega_n, \omega_0 \neq 2\omega_n$ as assumed). Kang & Leal (1988) obtained the same effect for a constant-volume bubble. The modified frequency $\Omega_n = \omega_n(1-Q_n\,\epsilon)$, is either increased or decreased, depending upon the physical properties (i.e. γ and ω_0) of the gas inside the bubble. For example, in the case of the $n=2$ deformation mode, $\Omega_2 = \omega_2(1-0.3093\epsilon)$ for a constant-volume bubble (i.e. $\omega_0 \to \infty$), while $\Omega_2 = \omega_2(1+0.0448\epsilon)$ for $\omega_0 = 10$. The limiting result for a constant-volume bubble is nearly identical to that obtained earlier by Kang & Leal (1988) in which the purely imaginary eigenvalue λ_2 was directly calculated as $\lambda_2 = \omega_2(1-0.31\epsilon)\,\mathrm{i}$. It is also noteworthy that the natural frequency ω_n decreases as the amplitude increases.

An important objective of the present theory is the pressure disturbance at large distances from the bubble owing to the volume and shape oscillations. The disturbance pressure at infinity corresponding to the shape and volume oscillations

defined by the solutions (5.18) and (5.11)–(5.13) can be determined via (4.11). The result, correct to $O(\epsilon^{\frac{3}{2}})$, is

$$P^{\infty} = \epsilon\left[A_0\,\omega_0 \sin\{\omega_0(1-Q_0\,\epsilon)\,t\}\frac{1}{r}+O\left(\frac{A_2}{r^3}\right)+\epsilon^{\frac{3}{2}}\left[A_0\cos\{\omega_0(1-Q_0\,\epsilon)\,t\}P_2(\eta)\right.\right.$$

$$\left.\left.-\frac{A_2}{(\omega_2^2-\omega_0^2)}\{\omega_0^2\cos\omega_0\,t-\omega_2^2\cos\{\omega_2(1-Q_2\,\epsilon)\,t\}\right]\frac{1}{r}+O(\epsilon^2)\quad \text{as } r\to\infty. \quad (5.20)$$

Thus, a monopole pressure disturbance (i.e. $1/r$) exists at both $O(\epsilon)$ and $O(\epsilon^{\frac{3}{2}})$.

The monopole pressure disturbance at $O(\epsilon)$ is clearly due to the radial (breathing) mode of oscillation at $O(\epsilon)$ that is created by the radially symmetric impulse in the pressure, $\epsilon A_0\,\delta(t)$. The monopole pressure contribution at $O(\epsilon^{\frac{3}{2}})$, on the other hand, has two distinct sources. The first is the standard 'Bernoulli' pressure, proportional at $O(\epsilon^{\frac{3}{2}})$ to the product of the undisturbed velocity $\nabla\phi_0$ and the $O(\epsilon)$ perturbation to the velocity $\nabla\phi_1$. The second is the contribution from the rate of change of local inertia at $O(\epsilon^{\frac{3}{2}})$, i.e. $\epsilon^{\frac{3}{2}}\partial\phi_{2,0}/\partial t$.

Of particular interest is the result obtained by considering the special case $A_0 = 0$, in which the bubble initially exhibits only shape oscillation at $O(\epsilon)$. It is obvious from (5.20) that the P_2-mode of deformation at $O(\epsilon)$ generates a monopole pressure disturbance at $O(\epsilon^{\frac{3}{2}})$, which is due essentially to the presence of the external flow. Specifically, in the absence of the external flow, we have seen in §4.1 that a deformation mode at $O(\epsilon)$ emits a monopole radiation only at $O(\epsilon^2)$, provided that we omit the special case $\omega_0 = 2\omega_n$ of mode–mode resonance. The result (5.20) therefore corroborates the earlier statement that the energy transfer from the deformation mode to the breathing mode of oscillation is very significantly enhanced by the presence of the external flow. It is especially noteworthy that the amount of energy the breathing mode gains at the expense of the deformation mode is rapidly increased when the two modes become nearly resonant in the limit as $\omega_0 \to \omega_2$.

As noted earlier, if $\omega_0 = \omega_2$ the bubble motion will exhibit a resonance between the radial 'breathing' mode and the P_2-mode of shape deformation at $O(\epsilon^{\frac{3}{2}})$. This resonant interaction is responsible for the rapid growth of the monopole radiation intensity at $O(\epsilon^{\frac{3}{2}})$ as $\omega_0 \to \omega_2$ (and the rapid growth which would occur at $O(\epsilon^2)$ if we calculated P^{∞} to that level as $\omega_0 \to \omega_n$ or $\omega_0 \to 2\omega_n$). In the following, we consider the special cases involving resonant interaction in detail, beginning with the resonant interaction between the radial and P_2 modes that occurs at $O(\epsilon^{\frac{3}{2}})$ when $\omega_0 = \omega_2$.

5.2. *Resonant interaction at* $O(\epsilon^{\frac{3}{2}})$ *when* $\omega_0 = \omega_2$

Let us then consider the special case, when $\omega_0 = \omega_2$. In fact, we can see from (5.7)–(5.9) or (5.14)–(5.16) that secular terms (and resonant interactions) actually occur at both $O(\epsilon^{\frac{3}{2}})$ and $O(\epsilon^2)$ when $\omega_0 = \omega_2$. The difference is that the $O(\epsilon^{\frac{3}{2}})$ resonance influences the amplitude function $\alpha_{1,n}$ on the timescale $\epsilon^{\frac{1}{2}}t$, and the one at $O(\epsilon^2)$ only appears on the much longer timescale ϵt. In this section, we consider only the effects at $O(\epsilon^{\frac{3}{2}})$. This secularity at $O(\epsilon^{\frac{3}{2}})$ (i.e. the terms containing $\exp(i\omega_2 t)$ and $\exp(i\omega_0 t)$ in (5.7) and (5.8), respectively) is generated by interactions between the undisturbed streaming flow (i.e. $\phi_0 = O(\epsilon^{\frac{1}{2}})$) and the oscillations of bubble volume and shape at $O(\epsilon)$. Perhaps the most important difference between the present case, and the resonant mode–mode interactions discussed earlier for a quiescent fluid, is that it occurs on the much shorter timescale $\epsilon^{\frac{1}{2}}t = O(1)$ rather than $\epsilon t = O(1)$. This suggests that viscous damping (to be considered in a subsequent paper) will play a much less

important role in inhibiting the growth of resonant modes in the presence of flow, than it does for a quiescent fluid.

In this case, the condition to preclude the appearance of secularity can be easily seen from (5.7) and (5.8) to be

$$\frac{\partial \alpha_{1,0}}{\partial \zeta} = -\tfrac{1}{6}\alpha_{1,2}, \tag{5.21}$$

$$\frac{\partial \alpha_{1,2}}{\partial \zeta} = +\tfrac{5}{2}\alpha_{1,0}. \tag{5.22}$$

The solution of these equations, which incorporates the initial condition $\alpha_{1,n}(0) = \mathrm{i}A_n(n+1)/\omega_n$, is

$$\alpha_{1,0}(\zeta) = \mathrm{i}\frac{(A_0^2+\frac{3}{5}A_2^2)^{\frac{1}{2}}}{\omega_0}\cos[(\tfrac{5}{12})^{\frac{1}{2}}\zeta+\Delta], \tag{5.23}$$

$$\alpha_{1,2}(\zeta) = \mathrm{i}\frac{3(\frac{5}{3}A_0^2+A_2^2)^{\frac{1}{2}}}{\omega_2}\sin[(\tfrac{5}{12})^{\frac{1}{2}}\zeta+\Delta], \tag{5.24}$$

where the phase angle Δ is given by

$$\Delta = \tan^{-1}\left(\frac{(15)^{\frac{1}{2}}A_2}{5A_0}\right). \tag{5.25}$$

Then the complete solution for the resonant case ($\omega_0 = \omega_2$) at $O(\epsilon^{\frac{3}{2}})$ can be expressed as

Radial mode

$$a_{1,0}(t) = a_{1,0}^s - \frac{(A_0^2+\frac{3}{5}A_2^2)^{\frac{1}{2}}}{\omega_0}\cos(\epsilon^{\frac{1}{2}}(\tfrac{5}{12})^{\frac{1}{2}}t+\Delta)\sin\omega_0 t, \tag{5.26}$$

$$\phi_{1,0}(t,r,\eta) = (A_0^2+\tfrac{3}{5}A_2^2)^{\frac{1}{2}}\cos(\epsilon^{\frac{1}{2}}(\tfrac{5}{12})^{\frac{1}{2}}t+\Delta)\cos\omega_0 t\frac{1}{r}. \tag{5.27}$$

P_2 mode

$$a_{1,2}(t) = a_{1,2}^2 - \frac{3(\frac{5}{3}A_0^2+A_2^2)^{\frac{1}{2}}}{\omega_2}\sin(\epsilon^{\frac{1}{2}}(\tfrac{5}{12})^{\frac{1}{2}}t+\Delta)\sin\omega_2 t, \tag{5.28}$$

$$\phi_{1,2}(t,r,\eta) = (\tfrac{5}{3}A_0^2+A_2^2)^{\frac{1}{2}}\sin(\epsilon^{\frac{1}{2}}(\tfrac{5}{12})^{\frac{1}{2}}t+\Delta)\cos\omega_2 t\frac{P_2(\eta)}{r^3}. \tag{5.29}$$

The solutions for the other modes ($n \neq 0, 2$) are not changed and remain as in (5.18) and (5.19). This latter observation leads to the obvious question as to why the resonant coupling at $O(\epsilon^{\frac{3}{2}})$ involves only P_2 and not additional shape deformation modes. At first glance, it seems obvious that this must be a consequence of the P_2 symmetry of the mean flow, (3.1). The only caveat to this conclusion is the observation that the first approximation to the steady deformed bubble shape involves both P_2 and P_4, thus perhaps suggesting that the situation is somewhat more complicated than it might first appear. In any case, we believe that a resonant coupling would exist between any mean flow that leads to bubble deformation, and oscillations of volume that will lead to time-dependent oscillations of shape of equal amplitude. It is only the particular resonantly-driven shape mode (or modes) that would change if the form of the mean flow is changed.

The main observation from the solution (5.26)–(5.29) is that the multiple-scale

analysis predicts the existence of slowly oscillating amplitudes $\cos(5\epsilon/12)^{\frac{1}{2}}t+\Delta$ and $\sin(5\epsilon/12)^{\frac{1}{2}}t+\Delta$ for the radial and P_2 modes of deformation, respectively. An important additional qualitative feature of the solution (5.26)–(5.29) is that resonant mode coupling exists between the radial and P_2 modes for all combinations of $A_0 \neq 0$ and/or $A_2 \neq 0$. We have seen previously that mode coupling (either resonant or non-resonant) exists in the absence of flow only if there is an initial perturbation of the bubble shape. Specifically, in the absence of flow, purely radial oscillations at $t = 0$ do not lead to oscillations of shape. On the other hand, in the presence of a deforming mean flow, we found in the non-resonant case that an initial radial oscillation at $O(\epsilon)$ could induce a shape oscillation at $O(\epsilon^{\frac{3}{2}})$. The present solution, (5.26)–(5.29), shows that this new mode of coupling is enhanced for the P_2 mode via resonance, so that an initial impulse at $O(\epsilon)$ in either the volume or the P_2 mode of deformation produces an oscillation in the other mode, also at $O(\epsilon)$, and thence to a continuously sustained energy exchange between the modes for all time.

The mechanism for generating shape oscillations from an initial impulse in volume in the present case is simply that a bubble which oscillates radially is subjected to flow of different strengths as it changes radius, and the natural tendency of the flow to deform the bubble thus contributes a time-dependent shape. If the volume oscillations are driven at the natural frequency of the P_2 mode, there is a resonant growth in the amplitude of the P_2-mode oscillations. The possibility of large-amplitude oscillations of shape, driven by time-dependent changes in the spherically symmetric contribution to the pressure, may be an important factor in high-Reynolds-number bubble break-up phenomena. A final contrast between the present case and the bubble response to a pressure impulse without a mean flow is the continuous interchange of energy between the radial and shape modes. This is similar to the result obtained in a quiescent fluid (at resonance) due to a step change in the ambient pressure. In contrast, the resonant response to an impulsive change in pressure in the absence of flow ($\omega_0 = 2\omega_n$) always led to a one-way transfer of energy, from the deformation mode to the radial breathing mode.

The monopole pressure disturbance due to the bubble oscillation in the present resonant case (i.e. with flow and $\omega_0 = \omega_2$) can be shown to take the form

$$rP^{\infty}(t) = \epsilon\omega_0(A_0^2+\tfrac{3}{5}A_2^2)^{\frac{1}{2}}\cos\{\epsilon^{\frac{1}{2}}(\tfrac{5}{12})^{\frac{1}{2}}t+\Delta\}\sin\omega_0 t+O(\epsilon^{\frac{3}{2}}) \tag{5.30}$$

which is $O(\epsilon)$ even when $A_0 = 0$, i.e. the case in which the initial pressure impulse at the bubble surface does not have a radially symmetric component. Thus, when the radial mode and the P_2 deformation mode are in resonance, a deformation mode at $O(\epsilon)$ will create a monopole radiation at $O(\epsilon)$ owing to the continuous energy exchange between the two modes.

5.3. *Resonant interactions at $O(\epsilon^2)$ for $\omega_0 = \omega_n$*

Finally, let us turn to the resonant interactions at $O(\epsilon^2)$. We begin with the case where $\omega_0 = \omega_n$. In this case, secular terms appear in the governing equations (5.14)–(5.16) at $O(\epsilon^2)$ owing both to mode–mode interactions and to the existence of a frequency shift due to the non-spherical steady-state shape in the straining flow. We may note that one special case occurs, for $\omega_0 = \omega_2$, in which resonance appears for both the $O(\epsilon^{\frac{3}{2}})$ and $O(\epsilon^2)$ problems. However, the analysis of the effect at $O(\epsilon^2)$ in this case is independent of the analysis at $O(\epsilon^{\frac{3}{2}})$ because the response occurs on different timescales, $O(\epsilon t)$ here and $O(\epsilon^{\frac{1}{2}}t)$ in the previous case.

The analysis at $O(\epsilon^2)$ is somewhat more complicated because we must choose the slowly varying functions $\alpha_{1,n}$ to eliminate both the 'self-induced' and mode–mode

secularity terms simultaneously. This means that the frequency shift corresponding to the self-induced secularity will generally be different compared to that calculated earlier when $\omega_0 \neq \omega_n$, and we will also expect a slow variation of the amplitude of oscillation and/or the phase.

It is, perhaps, useful to consider a specific example to illustrate our case. Thus, let us suppose that $\omega_0 = \omega_4$ so that resonant interactions occur between the radial and P_4 shape deformation modes. In this case, to eliminate secular terms, we must choose $\alpha_{1,0}$ and $\alpha_{1,4}$ to set the first two terms on the right-hand sides of (5.14) and (5.16) equal to zero. Hence, we must choose the complex amplitude functions $\alpha_{1,0}$ and $\alpha_{1,4}$ to satisfy the conditions

$$\frac{\partial}{\partial \tau}\alpha_{1j} = \mathrm{i}\, C_{jk}\,\alpha_{1,k} \quad (j = 0,4, \quad k = 0,4), \tag{5.31}$$

where

$$C_{00} = \frac{373 - 1794\gamma}{2808\omega_4}, \quad C_{04} = -\frac{685}{1638\omega_4},$$

$$C_{40} = -\frac{3175}{182\omega_4}, \qquad C_{44} = -\frac{1\,973\,845}{386\,232\omega_4}.$$

By applying the initial conditions, we can solve (5.31) for $\alpha_{1,0}(\tau)$ and $\alpha_{1,4}(\tau)$. The resulting complete solution for $a_{1,0}$ and $a_{1,n}$ is given by

$$a_{1,0}(t) = a^{\mathrm{s}}_{1,0} + \frac{5A_4 C_{04} + (C_{00} - \lambda_1) A_0}{\omega_4(\lambda_1 - \lambda_2)} \sin\{(\omega_4 + \epsilon\lambda_2)\, t\}$$

$$- \frac{5A_4 C_{04} + (C_{00} - \lambda_2) A_0}{\omega_4(\lambda_1 - \lambda_2)} \sin\{(\omega_4 + \epsilon\lambda_1)\, t\}, \tag{5.32}$$

$$a_{1,4}(t) = a^{\mathrm{s}}_{1,4} + \frac{5A_4 C_{04} + (C_{00} - \lambda_1) A_0}{\omega_4(\lambda_1 - \lambda_2)\, C_{04}} (\lambda_2 - C_{00}) \sin\{(\omega_4 + \epsilon\lambda_2)\, t\}$$

$$- \frac{5A_4 C_{04} + (C_{00} - \lambda_2) A_0}{\omega_4(\lambda_1 - \lambda_2)\, C_{04}} (\lambda_1 - C_{00}) \sin\{(\omega_4 + \epsilon\lambda_1)\, t\}, \tag{5.33}$$

in which λ_1 and λ_2 are the eigenvalues of C_{jk} and defined as

$$\lambda_{1,2} \equiv \tfrac{1}{2}\{C_{00} + C_{44} \pm ((C_{00} - C_{44})^2 + 4C_{04}\, C_{40})^{\frac{1}{2}}\}. \tag{5.34}$$

We see that the solution to (5.31) produces both a slowly varying amplitude and a frequency shift. This is reflected in the analysis by the necessity of simultaneously eliminating the self-induced and regular mode–mode secularity terms.

The velocity field due to the bubble oscillation can be easily evaluated from the present solution (5.32)–(5.33), plus the solutions for the other oscillation modes ($n \neq 0, 4$) which remain unchanged from (5.18)–(5.19).

An interesting feature of the solution (5.32) and (5.33) is that the two modes continuously exchange their energy and thus sustain both modes of oscillation for all time. To see that this is true, we may again consider an example in which $A_0 = 0$. In this case, the shape oscillation at $O(\epsilon)$ will induce a radial mode oscillation at $O(\epsilon)$. The solution for the radial mode of oscillation can be expressed as

$$a_{1,0}(t) = \frac{10A_4 C_{12}}{\omega_4(\lambda_1 - \lambda_2)} \sin\left\{\frac{(\lambda_2 - \lambda_1)}{2}\tau\right\} \cos\left[\omega_0\left\{1 + \frac{\epsilon(\lambda_1 + \lambda_2)}{2\omega_0}\right\} t\right]. \tag{5.35}$$

Thus, the slowly varying amplitude is $\sin\{\frac{1}{2}(\lambda_2-\lambda_1)\tau\}$ and the frequency is modified as $\Omega_0 = \omega_0\{1+\epsilon(\lambda_1+\lambda_2)/2\omega_0\}$, which is a function of ϵ and γ. In fact, the frequency is monotonically decreased as ϵ and γ increase, i.e.

$$\Omega_0 = \begin{cases}\omega_0(1-0.01560\epsilon), & \gamma = 1.0,\\ \omega_0(1-0.01631\epsilon), & \gamma = 1.4.\end{cases}$$

5.4. *Resonant interactions at $O(\epsilon^2)$ for $\omega_0 = 2\omega_n$*

Finally, we consider the last resonant case when $\omega_0 = 2\omega_n$ owing to mode–mode interactions. In this case, it is again necessary to choose the slowly varying coefficients $\alpha_{1,n}$, in such a way that both the self-induced secular terms and the mode–mode secular terms are simultaneously cancelled. As in the previous example, this means that the mode–mode interactions not only produce a slow variation in the amplitude of oscillation, but also a modified frequency shift owing to the mean deformation. To be specific, we again illustrate results by considering a specific case, $\omega_0 = 2\omega_4$. Then, it can be seen from (5.14) and (5.16) that the conditions for elimination of secular behaviour are

$$\frac{\partial\alpha_{1,0}}{\partial\tau} = -\mathrm{i}B_1\alpha_{1,0} + \mathrm{i}B_2\alpha_{1,4}^2, \tag{5.36}$$

$$\frac{\partial\alpha_{1,4}}{\partial\tau} = -\mathrm{i}B_3\alpha_{1,4} + \mathrm{i}B_4\alpha_{1,4}^*\alpha_{1,0}, \tag{5.37}$$

where
$$B_1 = \frac{5\omega_2^2}{6(\omega_2^2-\omega_0^2)\omega_0} + \frac{15\gamma\omega_0^2+10(3\gamma-1)}{24\omega_0^3}, \quad B_2 = \frac{15}{4\omega_0},$$

$$B_3 = \frac{866225}{193116\omega_4} + \frac{225}{4\omega_0^2\omega_4}, \qquad B_4 = \frac{675}{2\omega_4},$$

with an initial condition $\alpha_{1,n}(0) = [(n+1)A_n]\mathrm{i}/\omega_n$. To facilitate the solution of these equations, we write the complex functions $\alpha_{1,0}$ and $\alpha_{1,4}$ in terms of their amplitude and phase

$$\alpha_{1,0} = \mathrm{i}M_0(\tau)\exp(\mathrm{i}\Theta_0(\tau)), \quad \alpha_{1,4} = \mathrm{i}M_4(\tau)\exp(\mathrm{i}\Theta_4(\tau)), \tag{5.38}$$

where M_0, M_4, Θ_0 and Θ_4 are real functions of τ. On substituting (5.38) into (5.36) and (5.37), we have

$$\frac{\partial M_0}{\partial\tau} = -B_2M_4^2\cos(2\Theta_4-\Theta_0), \quad \frac{\partial M_4}{\partial\tau} = B_4M_0M_4\cos(2\Theta_4-\Theta_0), \tag{5.39}$$

$$M_0\frac{\partial\Theta_0}{\partial\tau} = -B_1M_0 - B_2M_4^2\sin(2\Theta_4-\Theta_0), \quad \frac{\partial\Theta_4}{\partial\tau} = -B_3 - B_4M_0\sin(2\Theta_4-\Theta_0). \tag{5.40}$$

Then, the complete solutions for the radial mode of oscillation and the P_4 oscillation mode can be expressed as

$$a_{1,n}(t,\tau) = a_{1,n}^s - M_n(\tau)\sin\{\omega_n t+\Theta_n(\tau)\}, \tag{5.41}$$

$$\phi_{1,n}(t,\tau,r,\eta) = \frac{\omega_n}{n+1}M_n(\tau)\cos\{\omega_n t+\Theta_n(\tau)\}\frac{P_n(\eta)}{r^{n+1}}, \tag{5.42}$$

for $n = 0, 4$. The solutions for the other oscillation modes remain unchanged as in (5.18) and (5.19).

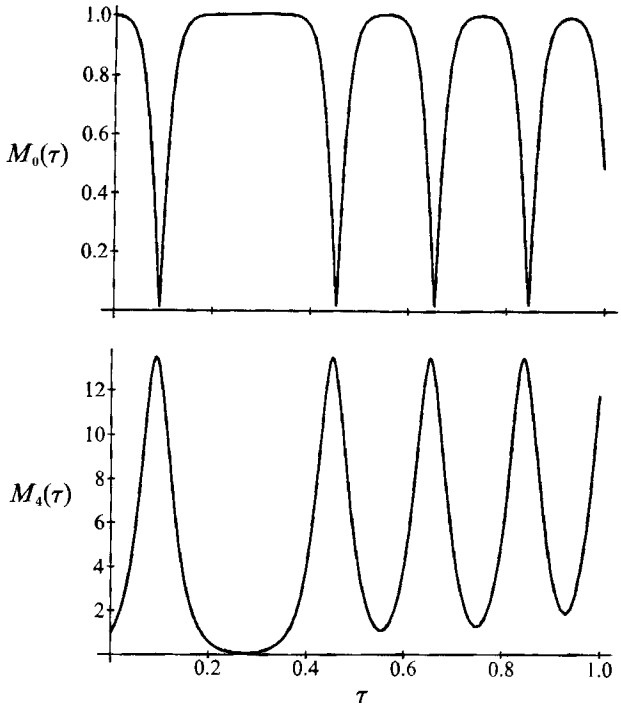

FIGURE 7. Amplitude modulations as a function of the slow timescale τ at the resonant state $\omega_0 = 2\omega_n$ for $n = 4$, $M_0(0) = M_4(0) = 1$ and $\gamma = 1$: (*a*) radial mode; (*b*) P_4-mode. The radial and P_4-mode oscillate about 30 and 15 cycles, respectively, during time interval $\Delta\tau = 1$ for $\epsilon = 0.1$.

In order to examine the energy transfer mechanism for this resonance case, we consider several different sets of the initial condition $(M_0(0), M_4(0))$.

Let us first consider the case for $M_0(0) = M_4(0) = 1$ (i.e. $A_n = \omega_n/(n+1)$; $n = 0,4$). The slowly varying amplitude functions M_0 and M_4 for this initial condition are plotted as a function of the slow timescale τ in figure 7. It can easily be seen that the two oscillation modes are sustained by exchanging their energy continuously. This is quite different behaviour from the same case for a quiescent fluid (i.e. $\omega_0 = 2\omega_n$) where it was found that all of the initial energy of the shape deformation mode is eventually transferred to the radial mode. Further, as shown in figure 8, the two resonant modes experience a phase modulation which is not present in the absence of an external flow. The magnitudes of the phase modulation increase with τ for both of the modes. More interestingly, when one oscillation mode undergoes phase modulation, the other mode oscillates without any phase change. This can be seen in figure 9 in which the phase diagram, Θ_4 *vs.* Θ_0, is plotted.

In figures 10 and 11 the phase diagrams, (M_0, M_4) and (Θ_0, Θ_4) are plotted for $M_0(0) = 0, M_4(0) = 1$. In this case each mode undergoes both an amplitude modulation on the periodic orbit $ABACA\ldots$ in the phase plane (M_0, M_4) and a phase modulation. It is thus obvious that a bubble which initially executes a P_4 mode oscillation at $O(\epsilon)$ can create a radial mode at the same order, $O(\epsilon)$, and each mode is sustained continuously. On the other hand, it can be noted from (5.39) that when $M_4(0) = 0$ and $M_0(0) = 1$, $M_0(\tau) = 1$ and $M_4(\tau) = 0$ at all times. Thus, when a bubble initially executes only a radial mode oscillation at $O(\epsilon)$ owing to an isotropic impulse in pressure, it cannot create a P_4 oscillation at $O(\epsilon)$. In this case, the leading-order solution for the P_4 mode occurs at $O(\epsilon^{\frac{3}{2}})$ and can be determined

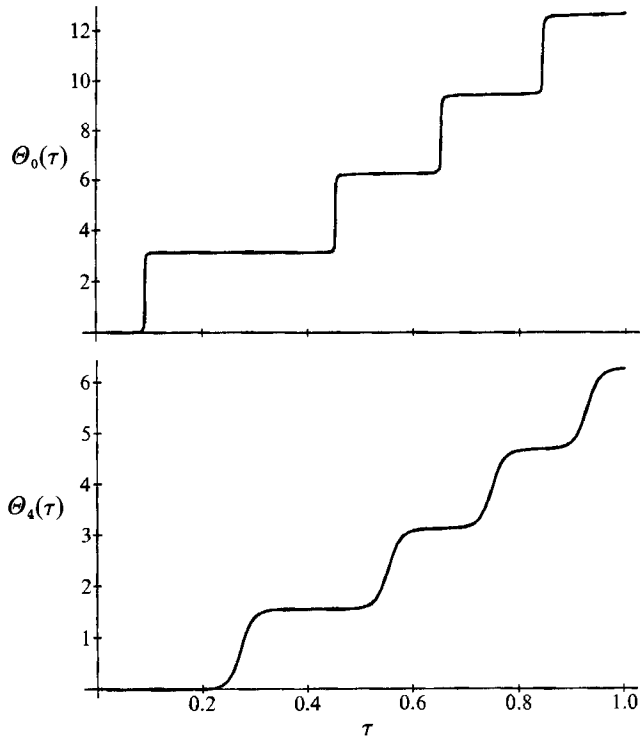

FIGURE 8. Phase modulations as a function of the slow timescale τ at the resonant state for the same set of parameters as in figure 7.

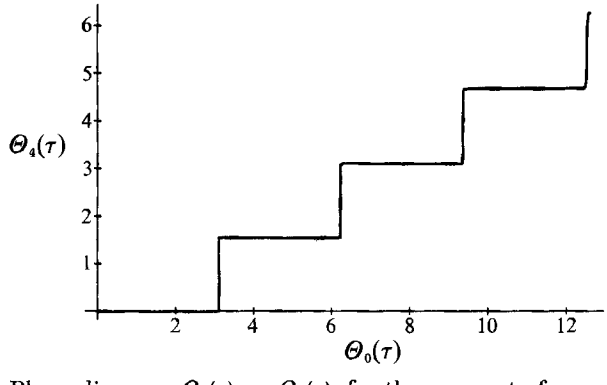

FIGURE 9. Phase diagram, $\Theta_4(\tau)$ *vs.* $\Theta_0(\tau)$, for the same set of parameters as in figure 7.

from (5.13). This result is different from that obtained for the resonant case at either $O(\epsilon^{\frac{3}{2}})$ when $\omega_0 = \omega_2$ or at $O(\epsilon^2)$ when $\omega_0 = \omega_n$. In the latter cases, one mode of oscillation at $O(\epsilon)$ always creates the other mode of oscillation at the same order.

In figure 12, the phase portraits, $M_4(\tau)$ *vs.* $M_0(\tau)$, for various sets of initial conditions $\{M_0(0), M_4(0)\}$ are plotted. When $\omega_0 = 2\omega_4$, the ideal-gas bubble in the presence of the straining flow continuously executes the radial and P_4-deformation oscillation, on the periodic orbit in the phase plane unless $M_4(0) = 0$, in which case the bubble exhibits only the radial mode oscillation at all times. This is qualitatively different from the result obtained for a quiescent fluid (see figure 3). In that case, the

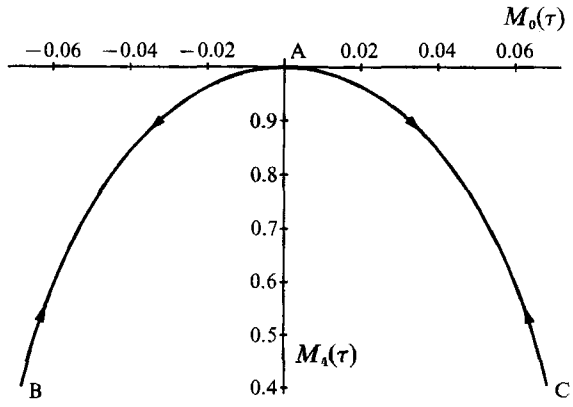

FIGURE 10. Phase diagram, $M_4(\tau)$ *vs.* $M_0(\tau)$, for $n = 4$, $M_0(0) = 0$, $M_4(0) = 1$, and $\gamma = 1$.

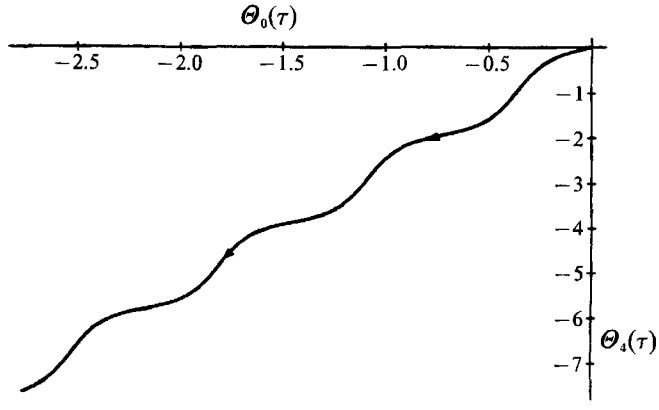

FIGURE 11. Phase diagram, $\Theta_4(\tau)$ *vs.* $\Theta_0(\tau)$, for the same set of parameters as in figure 10.

shape oscillation loses its energy to the radial mode and eventually decays exponentially. On the other hand, in the presence of the ambient straining flow, the bubble shape cannot be spherical at all times owing to the non-uniform pressure distribution imposed by the external flow. The existence of a non-spherical steady-state shape leads to the qualitatively new effect described above.

Finally, it is noteworthy that the general features of the results discussed in this section for bubble oscillations caused by an impulsive change in the pressure in the presence of a uniaxial flow, are not altered if we consider a step change in pressure, i.e. (4.26). For the step change, the leading-order solution is given by

$$a_{1,n}(t,\zeta,\tau) = \frac{1}{2}\left\{\alpha_{1,n}(\tau,\zeta)\exp(\mathrm{i}\omega_n t) + a^{\mathrm{s}}_{1,n} - \frac{(n+1)A_n}{\omega_n^2}\right\} + \text{c.c.}, \tag{5.43}$$

$$\phi_{1,n}(t,\tau,\zeta,r,\eta) = -\frac{\mathrm{i}\omega_n}{2(n+1)}\alpha_{1,n}(\zeta,\tau)\exp(\mathrm{i}\omega_n t)\frac{P_n(\eta)}{r^{n+1}} + \text{c.c.}, \tag{5.44}$$

with

$$\alpha_{1,n}(0,0) = \frac{(n+1)A_n}{\omega_n^2}, \tag{5.45}$$

instead of (5.4)–(5.6) for the impulse. Thus, the bubble oscillates around a new steady-state shape $a^{\mathrm{s}}_{1,n} - (n+1)A_n/\omega_n^2$ with an amplitude $(n+1)A_n/\omega_n^2$.

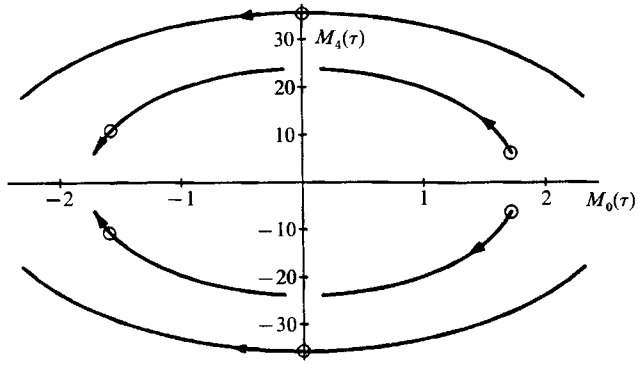

FIGURE 12. Phase diagram, $M_4(\tau)$ *vs.* $M_0(\tau)$, for various sets of initial conditions $\{M_0(0), M_4(0)\}$: ○, initial point and the arrows indicate the initial direction of the periodic orbits.

6. Conclusion

Small-amplitude oscillations of a bubble in an inviscid fluid have been studied using the standard method of domain perturbations. This analysis has led to the following conclusions.

The steady-state analysis shows that the existence of a barrel-like steady-state shape at the leading order of approximation is independent of the inclusion of bubble compressibility. The steady-state solution also demonstrates the existence of a limit point at a critical Weber number beyond which no solution exists on the branch of steady solutions that includes the spherical equilibrium state in the absence of the extensional flow. Furthermore, the critical Weber number for existence of a stable-steady solution is monotonically increased as the natural frequency ω_0 of the radial mode of oscillation increases. Thus, a gas bubble becomes less stable as the compressibility increases.

The analysis of small-amplitude oscillation caused by an impulsive or step change in the pressure at the bubble surface shows that the bubble motion can exhibit a resonant response owing to interactions between the deformation and radial modes of oscillation, and may also exhibit a frequency change when the bubble is either deformed or expanded/compressed away from its initial equilibrium volume.

In the absence of the straining flow, resonance takes place only at $O(\epsilon^2)$ for an ideal-gas bubble when $\omega_0 = 2\omega_n$ in the presence of an impulsive pressure change and when either $\omega_0 = \omega_n$ or $\omega_0 = 2\omega_n$ owing to a step change in the ambient pressure. The response analysis to the impulse in pressure predicts slowly varying amplitude envelopes that correspond to one-way energy transfer from the deformation mode to the radial mode of oscillation when $\omega_0 = 2\omega_n$. On the other hand, the bubble dynamics in response to a step change in the pressure exhibits, in general, a continuous exchange of energy when either $\omega_0 = \omega_n$ or $\omega_0 = 2\omega_n$ because the bubble oscillates around a non-equilibrium volume and a non-spherical steady-state shape owing to the modified pressure distribution on the bubble surface.

In the presence of a uniaxial straining flow, the self-induced secularity always arises at $O(\epsilon^2)$ from the non-spherical deformed shape, and a shape oscillation at $O(\epsilon)$ induced by a pressure change at the same order will generate a radial mode of oscillation at $O(\epsilon^{\frac{3}{2}})$ which is considerably stronger than the result [i.e. $O(\epsilon^2)$] obtained in the absence of the flow. On the other hand, when $\omega_0 = \omega_2$, resonance occurs at $O(\epsilon^{\frac{3}{2}})$ owing to the interaction of the volume oscillation at $O(\epsilon)$ and the undisturbed

extensional flow at $O(\epsilon^{\frac{1}{2}})$. In this case, a shape deformation at $O(\epsilon)$ will create a radial mode of oscillation of $O(\epsilon)$, and vice versa. Further, when either $\omega_0 = \omega_n$ or $\omega_0 = 2\omega_n$, resonance appears at $O(\epsilon^2)$ owing to the combined effects of mode–mode interactions and the existence of the non-spherical steady-state shape in the straining flow. For both resonance cases, the shape deformation mode is sustained continuously by exchanging energy with the radial mode, and we find not only the slowly varying amplitude indicated above, but also a phase modulation. Further, in the presence of flow, the general features of the solution are not altered when we replace an impulse in the pressure by a step change.

The present work was performed at the University of California, Santa Barbara during Professor Yang's leave in 1990–91 under partial support of the Korea Science and Engineering Foundation. The work has also been supported by grants to L. G. Leal from the Fluid Dynamics Programs at ONR and NSF.

REFERENCES

BACH, P. & HASSAGER, O. 1985 An algorithm for the use of Lagrangian specification in Newtonian fluid mechanics and applications to free-surface flow. *J. Fluid Mech.* **152**, 173–190.

BENJAMIN, T. B. 1989 Note on shape oscillations of bubbles. *J. Fluid Mech.* **203**, 419–424.

DOWLING, A. P. & FFOWCS WILLIAMS, J. E. 1983 *Sound and Sources of Sound.* Halsted.

FFOWCS WILLIAMS, J. E. & GUO, Y. P. 1991 On resonant nonlinear bubble oscillations. *J. Fluid Mech.* **224**, 507–529.

HALL, P. & SEMINARA, G. 1980 Nonlinear oscillations of non-spherical cavitation bubbles in acoustic fields. *J. Fluid Mech.* **101**, 423–444.

KANG, I. S. & LEAL, L. G. 1987 Numerical solution of axisymmetric, unsteady free-boundary problems at finite Reynolds number. I. Finite-difference scheme and its application to the deformation of a bubble in a uniaxial straining flow. *Phys. Fluids* **30**, 1929 1940.

KANG, I. S. & LEAL, L. G. 1988 Small-amplitude perturbations of shape for a nearly spherical bubble in an inviscid straining flow (steady shape and oscillatory motion). *J. Fluid Mech.* **187**, 231–266.

KANG, I. S. & LEAL, L. G. 1990 Bubble dynamics in time-periodic straining flows. *J. Fluid Mech.* **218**, 41–69.

LONGUET-HIGGINS, M. S. 1989*a* Monopole emission of sound by asymmetric bubble oscillations. Part 1. Normal modes. *J. Fluid Mech.* **201**, 525–541.

LONGUET-HIGGINS, M. S. 1989*b* Monopole emission of sound by asymmetric bubble oscillations. Part 2. An initial-value problem. *J. Fluid Mech.* **201**, 543–565.

LONGUET-HIGGINS, M. S. 1989*c* Some integral theorems relating to the oscillations of bubbles. *J. Fluid Mech.* **204**, 159–166.

LONGUET-HIGGINS, M. S. 1990 Bubble noise spectra. *J. Acoust. Soc. Am.* **87**, 652–661.

LONGUET-HIGGINS, M. S. 1991 Resonance in nonlinear bubble oscillations. *J. Fluid Mech.* **224**, 531–549.

MARSTON, P. L. 1980 Shape oscillation and static deformation of drops and bubbles driven by modulated radiation stress – Theory. *J. Acoust. Soc. Am.* **67**, 15–26.

MARSTON, P. L. & APFEL, R. E. 1979 Acoustically forced shape oscillation of hydrocarbon drops levitated in water. *J. Colloid Interface Sci.* **68**, 280–286.

MEDWIN, H. & BEAKY, M. M. 1989 Bubble sources of the Knudsen sea noise spectra. *J. Acoust. Soc. Am.* **86**, 1124–1130.

MIKSIS, M. 1981 A bubble in an axially symmetric shear flow. *Phys. Fluids* **24**, 1129–1231.

PLESSET, M. S. & PROSPERETTI, A. 1977 Bubble dynamics and cavitation. *Ann. Rev. Fluid Mech.* **9**, 145–185.

PROSPERETTI, A. 1984 Bubble phenomena in sound fields: part 2. *Ultrasonics*, May, 115–124.

Prosperetti, A. & Lu, N. Q. 1988 Cavitation and bubble bursting as sources of oceanic ambient noise. *J. Acoust. Soc. Am.* **84**, 1037–1041.

Ryskin, G. & Leal, L. G. 1984 Numerical solutions of free-boundary problems in fluid mechanics. Part 3. Bubble deformation in an axisymmetric straining flow. *J. Fluid Mech.* **148**, 37–43.

Subramanyam, S. V. 1969 A note on the damping and oscillations of a fluid drop moving in another fluid. *J. Fluid Mech.* **37**, 715–725.

Yosioka, K. & Kawasima, Y. 1955 Acoustic radiation pressure on a compressible sphere. *Acoustica* **5**, 167–173.